MARTIN MARIETTA ENERGY SYSTEMS LIBRARIES
3 4456 0361506 9

CENTRAL RESEARCH LIBRARY
DOCUMENT COLLECTION

ORNL-2962
UC-25 – Metals, Ceramics, and Materials
(TID-4500 17th ed.)

58

IN-PILE LOOP INVESTIGATIONS OF CORROSION OF ZIRCALOY-2 AND OTHER POSSIBLE REACTOR MATERIALS IN 0.04 *m* UO_2SO_4 AT 280°C

G. H. Jenks
J. E. Baker

CENTRAL RESEARCH LIBRARY
DOCUMENT COLLECTION
LIBRARY LOAN COPY
DO NOT TRANSFER TO ANOTHER PERSON
If you wish someone else to see this document, send in name with document and the library will arrange a loan.

OAK RIDGE NATIONAL LABORATORY
operated by
UNION CARBIDE CORPORATION
for the
U.S. ATOMIC ENERGY COMMISSION

Printed in USA. Price $1.25 . Available from the

Office of Technical Services
U. S. Department of Commerce
Washington 25, D. C.

LEGAL NOTICE

This report was prepared as an account of Government sponsored work. Neither the United States, nor the Commission, nor any person acting on behalf of the Commission:

A. Makes any warranty or representation, express or implied, with respect to the accuracy, completeness, or usefulness of the information contained in this report, or that the use of any information, apparatus, method, or process disclosed in this report may not infringe privately owned rights; or

B. Assumes any liabilities with respect to the use of, or for damages resulting from the use of any information, apparatus, method, or process disclosed in this report.

As used in the above, "person acting on behalf of the Commission" includes any employee or contractor of the Commission to the extent that such employee or contractor prepares, handles or distributes, or provides access to, any information pursuant to his employment or contract with the Commission.

ORNL-2962

Contract No. W-7405-eng-26

REACTOR CHEMISTRY DIVISION

IN-PILE LOOP INVESTIGATIONS OF CORROSION OF ZIRCALOY-2 AND OTHER POSSIBLE REACTOR MATERIALS IN 0.04 *m* UO_2SO_4 AT 280°C

G. H. Jenks J. E. Baker

DATE ISSUED

APR 23 1962

OAK RIDGE NATIONAL LABORATORY
Oak Ridge, Tennessee
operated by
UNION CARBIDE CORPORATION
for the
U. S. ATOMIC ENERGY COMMISSION

MARTIN MARIETTA ENERGY SYSTEMS LIBRARIES

3 4456 0361506 9

CONTENTS

ABSTRACT 1

1. INTRODUCTION 2

2. EQUIPMENT AND CONSTRUCTION 2

3. OPERATION 5
   - 3.1 Out-of-Pile Pretreatment 5
   - 3.2 In-Pile Operation 5
   - 3.3 Dismantling 9

4. RESULTS AND EVALUATION 11
   - 4.1 Out-of-Pile 11
   - 4.2 In-Pile 11
   - 4.3 Qualitative Inspection of Loop 23
   - 4.4 Metallographic Examinations 26
   - 4.5 Quantitative Inspection of Loop 26

5. SUMMARY AND DISCUSSION OF RESULTS 35
   - 5.1 Zircaloy-2 35
   - 5.2 Titanium-55A 37
   - 5.3 Stainless Steel 38
   - 5.4 Solution Stability 40

REFERENCES 41

IN-PILE LOOP INVESTIGATIONS OF CORROSION OF ZIRCALOY-2 AND OTHER POSSIBLE REACTOR MATERIALS IN 0.04 m UO_2SO_4 AT 280°C

G. H. Jenks J. E. Baker

ABSTRACT

In-pile loop experiment L-2-10 was one of a series designed to test the radiation corrosion of Zircaloy-2 and other possible reactor construction materials in UO_2SO_4 solutions under various radiation intensities, temperatures, solution compositions, and velocities of flow past specimens. The solution employed was 0.04 *m* UO_2SO_4, 0.0075 *m* $CuSO_4$, and 0.02 *m* H_2SO_4 in H_2O. Radiation exposure was carried out in the LITR HB-2 facility, at a main-stream temperature of 280°C. Construction material for the loop was type 347 stainless steel. Specimens of Zircaloy-2, Ti-55A, platinum, and types 347 and 309 SCb stainless steel were tested. The power density at core specimens ranged from a maximum of 4.2 to a minimum of 0.8 w/ml. The total time of high-temperature operation with UO_2SO_4 solutions was 1872 hr, of which 1672 hr was with enriched UO_2SO_4. In-pile circulation time for this experiment (following the initial reactor startup) was 1456 hr, and the reactor energy was 3765 Mwhr, with most of the energy accumulated at the 3-Mw power level.

The over-all corrosion rate of steel in the loop decreased slightly with time of exposure. The average over-all steel rate based on oxygen data and radiation time was 0.47 mpy (mils per year). The average rate based on nickel data was less than 0.3 mpy, but the nickel results are believed to be low because of sorption of this material on corrosion product oxides.

The average and maximum rates for type 347 stainless steel channel specimens outside the core were 0.18 and 0.45 mpy, based on weight loss data, exposed-area attack, and radiation time. The comparably determined minimum and maximum rates for channel specimens in the core ranged from 0.1 to 2.8 mpy, with the rate increasing in an apparently regular fashion with increasing power density above about 2 w/ml. Below this power, the rates were about the same as those observed in-line. There was no apparent effect of varying solution velocities in the range 10 to 40 fps on either the core channel or in-line channel specimens.

Specimens of types 347 and 309 SCb stainless steel exposed on one assembly in the core annulus region corroded at much higher rates than core channel specimens, but annulus steel specimens on another similar array corroded at somewhat lower rates than the channel specimens. The explanation for this difference is unknown. Differences in galvanic action between the specimens located on each of the assemblies is considered the most likely explanation, but no detailed mechanism is suggested.

Zircaloy-2 corrosion results from this loop have been discussed and correlated elsewhere in terms of the 280°C relationship between corrosion rate R (mpy), power density P (w/ml), and uranium sorption factor α:

$$1/R = 2.23/P\alpha + 1/40 .$$

The data from this experiment obey this relationship. The value of α for core annulus specimens, which were exposed to a velocity of about 0.8 fps, was 6.9. For the exposed surfaces of those channel specimens located in the convergent section of the channel and exposed to average velocities of 19 and 33 fps, the best estimates of α are in the range 1 to 1.8. Specimens located in the divergent section of the channel exhibited higher α values.

Results for Ti-55A specimens indicate that in-pile titanium corrosion was affected by some uniform change in the solution under radiation to a greater extent than by fission recoil irradiation of specimen surfaces or by the fissioning taking place in the solution immediately adjacent to specimens. However, the result obtained with one core specimen exposed to the highest average solution velocity (35 fps) suggests that the susceptibility of this material to adverse velocity effects is increased by exposure to fissioning solution. With the exception of this one specimen, the average rate (based on radiation time and total area) for core channel specimens was 0.8 mpy, compared with an average of 0.7 mpy for in-line specimens. The similarly determined rate for the high-velocity specimen was 3.6 mpy.

Platinum corrosion was negligible.

There was no evidence of solution instability. Some discrepancies in analytical results were ascribed to sampling and analytical errors.

1. INTRODUCTION

In-pile loop experiment L-2-10 was one of a series designed to test the radiation corrosion of Zircaloy-2 and other possible reactor construction materials in UO_2SO_4 solutions under various radiation intensities, temperatures, solution compositions, and velocities of flow past specimens. The solution employed was 0.04 *m* UO_2SO_4, 0.0075 *m* $CuSO_4$, and 0.02 *m* H_2SO_4 in H_2O. Radiation exposure was made in the LITR HB-2 facility, and the main-stream temperature was 280°C. Previous loop experiments[1,2] had employed solutions 0.17 *m* in UO_2SO_4 and a main-stream temperature of 250°C. Also, the previous loops had been exposed in the LITR HB-4 facility, where the maximum thermal-neutron flux is less than that in HB-2 by a factor of 3 to 4.

Construction material for the loop was type 347 stainless steel. Specimens of Zircaloy-2, Ti-55A, platinum, and types 347 and 309 SCb stainless steel were tested.

The experiment was inserted in the reactor on July 2, 1956, and removed on September 3, 1956.

Results from this experiment have been previously summarized in the *Homogeneous Reactor Project Quarterly Progress Report for the Period Ending January 31, 1957* (ORNL-2272).

2. EQUIPMENT AND CONSTRUCTION

The structure of the loop and the equipment employed were similar to those reported for previous experiments.[3] The circulating pump was an ORNL 5-gpm model of the outboard-bearing type with pure sintered aluminum oxide bearings and journal bushings. Loop volumes and other specifications are given in Table 1.

The loop, constructed of type 347 stainless steel, contained four types of corrosion specimens in three locations. A tabulation of the specimen materials and types is given in Table 2. Identical sets of $\frac{1}{4} \times \frac{1}{2} \times 0.060$ in. corrosion coupons (24 each) in type 347 stainless steel tapered-channel coupon holders were installed in the core and in-line positions. Type 347 stainless steel, Zircaloy-2, and titanium-55A were used for these coupons and were arranged as shown in detail in Fig. 1. Six impact specimens of Zircaloy-2 were contained in the loop – three in the special line holder and three around the core coupon holder. Also, three tensile specimens of Zircaloy-2 and two rod-coupon assemblies were located in the core annulus and three tensile specimens of Zircaloy-2 were arranged in the special line holder in a manner similar to that of the impact specimens. The rod-coupons were $\frac{1}{2} \times \frac{1}{2} \times 0.060$ in. and were spaced

Table 1. Loop Volumes and Other Specifications for In-Pile Loop L-2-10

Loop volume (including pressurizer), ml	1508
Pressurizer volume, empty, ml	524
Core volume, empty, ml	372
Core volume, loaded, ml	300
Flow rates	
Pressurizer, cc/sec	7.4
Core, gpm	4.9
In-line, gpm	5.1
Pump bearing material	Al_2O_3
Pump journal material	Al_2O_3
System pressure checked at	
Hydraulic, psi	1300
Helium and leak detector, psi	500

Table 2. Number and Types of Corrosion Specimens in Experiment L-2-10

Specimens exposed in as-machined, as-received condition

Type	Tapered-Channel Coupon Holders		Rod-Coupon Assemblies (in core)		Tensile Specimens		Impact Specimens	
	Core	In-Line	Array A	Array B	Core	In-Line	Core	In-Line
347 SS	13	13	3	3				
309 SCb SS			2	2				
Zircaloy-2	5	5	2	2	3	3	3	3
Ti-55A	6	6						
Platinum			2	2				

evenly on 0.200-in.-diam rods. The rods, nuts, and spacers were of type 347 stainless steel. The coupons were fabricated of types 347 and 309 SCb stainless steel, Zircaloy-2, and platinum. Arrangement of the core impact, tensile, and annulus-coupon assemblies is shown in Fig. 2. Figure 3 shows the arrangement of specimens in the special line holder.

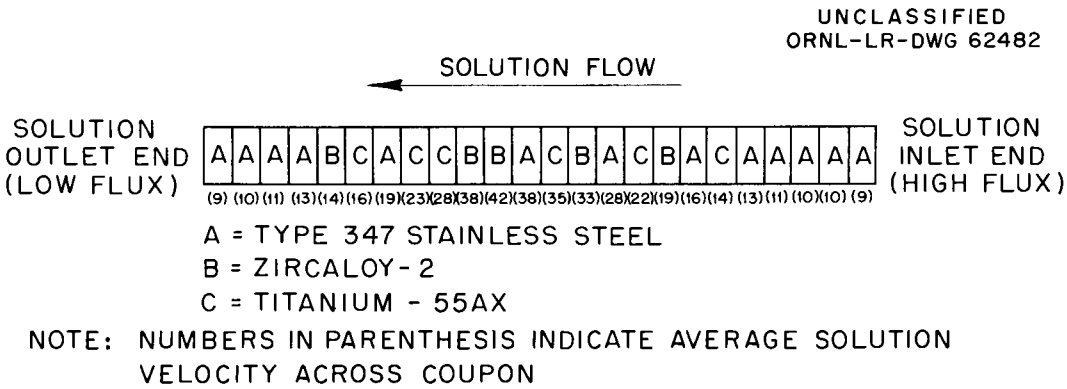

Fig. 1. Arrangement of Coupon Corrosion Specimens in the Core and In-Line Channel Holders.

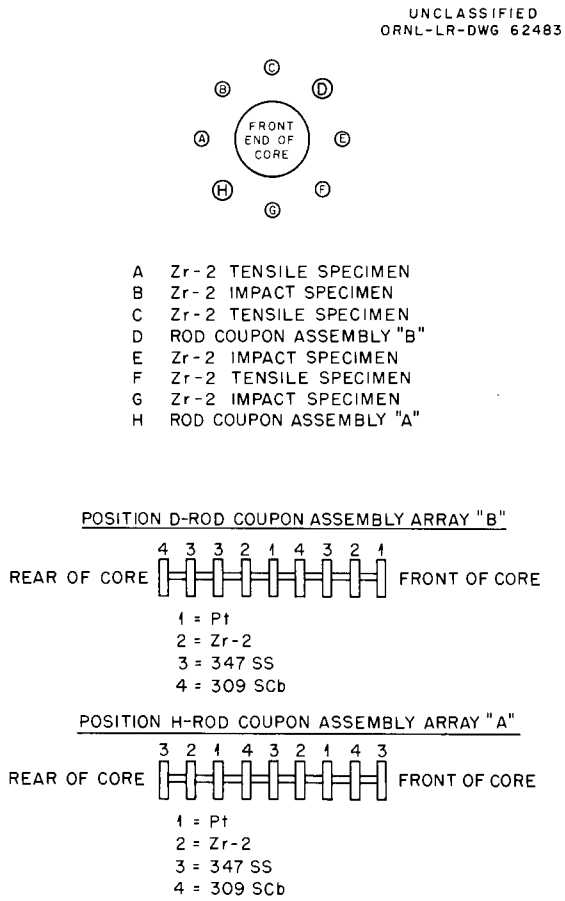

Fig. 2. Arrangement of Core Impact, Tensile, and Rod Coupons.

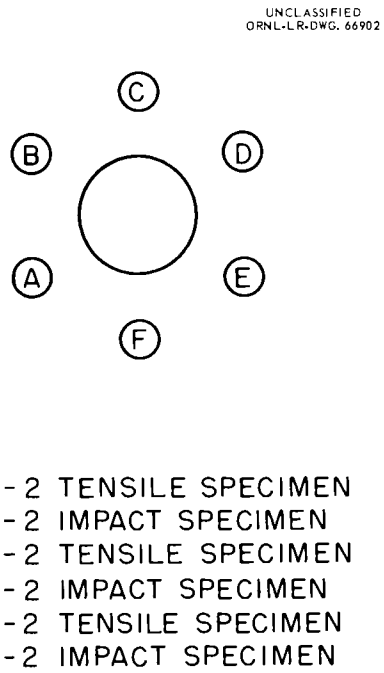

Fig. 3. Arrangement of Special-Line-Holder Specimens.

3. OPERATION

3.1 Out-of-Pile Pretreatment

During out-of-pile testing[3] the loop was operated for short periods with H_2O, solutions of trisodium phosphate, and solutions of HNO_3. The loop was also operated for 110 hr with a solution of 0.17 *m* UO_2SO_4 (natural), 0.04 *m* H_2SO_4, and 0.03 *m* $CuSO_4$ in H_2O. During the last run with H_2O, following the UO_2SO_4 run, the circulation pump failed. Examination of the pump revealed that the start windings on the stator were burned. Following replacement of the stator and a complete leak check of the loop, the loop was operated for a short period with H_2O and then for 90 hr with a solution of 0.04 *m* UO_2SO_4 (natural), 0.02 *m* H_2SO_4, and 0.0075 *m* $CuSO_4$ in H_2O. After a final H_2O run the loop was charged with an enriched-uranium solution and in-pile testing was begun. The loop preparatory operations are summarized in Table 3.

3.2 In-Pile Operation

The loop was charged with enriched-uranium solution and operated at temperature (280°C in the main stream and 305°C in the pressurizer) about 216 hr before the reactor was taken to power. The solution charged to the loop was 0.04 *m* UO_2SO_4, 0.0075 *m* $CuSO_4$, and 0.02 *m* H_2SO_4 in H_2O. A make-up solution, similar to the original but containing 0.044 *m* H_2SO_4 and 130 ppm Cr, was used to replace solution withdrawn as samples. Compositions of these solutions are shown in Table 4. The total circulation time with enriched solution was 1672 hr. The energy output of the LITR during this time was 3765 Mwhr, with essentially all the power liberated at the 3-Mw level. The reactor operating schedule for the exposure is shown in Fig. 4.

Table 3. Analyses of Samples from Loop Inventory During Preparatory Operations

Solution	Circulation Time for Each Solution (hr)	Inventory at Time of Sampling (ml)	Temperature (°C)		Uranium		Sulfate		Copper		Nickel		Iron		Chromium		Aluminum		Chlorine		pH
			Main-Stream	Pressurizer	Conc. (mg/ml)	Total (g)	Conc. (mg/ml)	Total (g)	Conc. (μg/ml)	Total (mg)	Conc. (μg/ml)	Total (mg)	Conc. (μg/ml)	Total (mg)	Conc. (μg/ml)	Total (mg)	Conc. (μg/ml)	Total (mg)	Conc. (μg/ml)	Total (mg)	
3% TSP (He)	5.5	1200	100	100							<1	<1	5	6	<1	<1	7	8	<1	<1	7.3
5% HNO_3(He)	21.5	1200	100	100					4	5	18	22	119	143	15	18			1	1	0.1
H_2O	22.3	1096	250	280					1	1.1	2	2	1	1	1	1			1	1	7.2
H_2O (O_2)	15.0	1096	250	280																	
H_2O (O_2)	6.0	1096	250	280																	
H_2O	16.4	1096	250	280																	
H_2O	5.1	1096	250	280																	
H_2O (O_2)	24.6	1096	300	315					<1	<1	5	6	<1	<1	3	3			7	8	4.6
H_2O	8.0	1096	250	280																	
0.17 *m* UO_2SO_4 (natural),	109.8	1096	250	280 (orig.)	38.8		23.4		2240		3		2		1		6		5		1.3
0.04 *m* H_2SO_4,					35.4	38.8	21.7	23.8	2070	2270	54	59	10	11	14	15			<2	<2	1.4
0.03 *m* $CuSO_4$ (O_2)					36.6	40.1	21.3	23.3	1980	2170	132	145	20	22	25	27			<1	<1	1.4
					33.0	36.2	21.3	23.3	1990	2180	217	238	37	41	14	15	15	16	<1	<1	1.3
				(final)	36.0	39.5	23.5	25.8	2050	2250	231	253	10	11	23	25	16	18	<2	<2	1.3
H_2O (He)	20.8	1100	250	280					2	2	<1	<1	2	2	<1	<1	<1	<1	<1	<1	3.5
H_2O (O_2)	12.3	1095	250	280																	
H_2O (O_2)	22.2	1100	250	280					<1	<1	<1	<1	<1	<1	7	8	<1	<1	<1	<1	3.4
Following Repairs																					
H_2O (O_2)	3.9	1116	250	280							<1	<1	<1	<1	<1	<1	<1	<1	<1	<1	5.2
0.04 *m* UO_2SO_4 (natural),	89.6	1015	280	305 (orig.)	10.1		7.0		490		<1		2		<1		19		2		1.5
0.02 *m* H_2SO_4,					9.4	9.7	7.0	7.1	490	497	7	7	7	7	3	3	31	31			1.6
0.0075 *m* $CuSO_4$ (O_2)					9.5	9.8	6.8	6.9	460	467	11	11	7	7	8	8	37	38	<2	<2	1.6
					9.9	10.0	7.0	7.1	510	518	17	17	38	39	13	13	13	13	2	2	1.5
					9.0	9.1	6.8	6.9	510	518	56	57	6	6	19	19	34	35	<2	<2	1.6
				(final)	9.6	9.7	6.4	6.5	460	467	25	25	5	5	21	21	15	15	<2	<2	1.9
H_2O	71.6	1010	250	280					0	0	1	1	1	1	18				<1	<1	3.5

Table 4. Analyses of Samples from Loop Inventory During Enriched-Solution Operation

Sample	Total Circulation Time (hr)	Accumulated LITR Energy (Mwhr)	Inventory Volume at Time of Sample, 25°C (ml)	Lithium[a] (mg/ml)	Sample Dilution Factor[b]	Uranium			Sulfate			Copper			Chromium		Nickel		Chlorine		Iron		Zirconium		Aluminum		Manganese		pH	Specific Gravity
						Rep (mg/ml)	Cor[c] (mg/ml)	Calcd[d] (mg/ml)	Rep (mg/ml)	Cor[e] (mg/ml)	Calcd[c] (mg/ml)	Rep (mg/ml)	Cor[d] (mg/ml)	Calcd[c] (mg/ml)	Rep (mg/ml)	Calcd Total[f] (g)	Rep (mg/ml)	Calcd Total[g] (g)	Rep (mg/ml)	Calcd Total[g] (g)	Rep (mg/ml)	Calcd Total[f] (g)	Rep (mg/ml)	Calcd Total[f] (g)	Rep (mg/ml)	Calcd Total[g] (g)	Rep (mg/ml)	Calcd Total[g] (g)		
Original charge			1024	0	1.0	10.4			7.1			0.49			0		0		0		0.02		0		0		0		1.7	1.02
Make-up solution				0	1.0	10.4			9.0			0.50			0.13		0		0		0.02		0		0		0		1.4	1.01
L-2-10-1[h]	28	0	1024	0.193	1.26	9.3	11.7	10.4	7.9	8.3	7.1	0.46	0.58	0.49			0.04	0.05	0	0	0.06	0.08	0	0	0	0	0	0	2.1	
L-2-10-2[h]	139	0	1027	0.271	1.41	8.5	11.9	10.4	8.2	8.9	7.1	0.58	0.82	0.49	0.15	0.22	0.06	0.10			0.21	0.31							1.9	
L-2-10-3[h]	184	0	1024	0.175	1.23	9.8	12.0	10.4	8.1	8.5	7.1	0.44	0.54	0.49	0.10	0.12	0.06	0.07			0.09	0.11							2.1	
L-2-10-4	256	112	1023	0.120	1.15	9.7	11.1	10.4	7.6	7.8	7.1	0.39	0.44	0.49	0.04	0.05	0.08	0.10	0	0	0.04	0.05							1.8	
L-2-10-5	280	170	1024	0.160	1.21	9.6	11.6	10.4	7.9	8.2	7.2	0.54	0.66	0.49	0.05	0.06	0.09	0.12			0.04	0.05							1.9	
L-2-10-6	352	378	1024	0.153	1.20	9.5	11.4	10.4	7.8	8.1	7.2	0.57	0.69	0.49	0.06	0.07	0.12	0.15			0.04	0.05							1.9	
L-2-10-7	520	708	1023	0.292	1.46	9.2	13.4	10.4	8.4	9.3	7.2	0.87	1.27	0.49	0.12	0.18	0.13	0.21			0.06	0.09					0	0	1.9	
L-2-10-8	592	886	1024	0.199	1.27	8.5	10.8	10.4	7.2	7.5	7.2	0.36	0.46	0.49	0.10	0.13	0.10	0.14			0.03	0.04			0	0			2.0	
L-2-10-9	688	1170	1023	0.192	1.27	9.3	11.8	10.4	7.9	8.3	7.2	0.40	0.50	0.49	0.13	0.16	0.11	0.15											1.9	
L-2-10-10	736	1294	1023	0.193	1.26	9.0	11.4	10.4	7.9	8.3	7.3	0.49	0.61	0.49			0.15	0.20			0.05	0.06	0.04	0.05					2.0	
L-2-10-11	784	1432	1023	0.190	1.26	9.4	11.8	10.4	7.8	8.2	7.3	0.52	0.66	0.49	0.17	0.22	0.24	0.32					0.03	0.04			0.01	0.01	2.0	
L-2-10-12	855	1622	1023	0.153	1.20	10.3	12.3	10.4	7.9	8.2	7.3	0.39	0.47	0.49	0.17	0.21	0.25	0.32											2.0	
L-2-10-13	924	1796	1023	0.186	1.25	9.3	11.6	10.4	8.0	8.5	7.3	0.41	0.52	0.49	0.09	0.12	0.22	0.28			0.04	0.05	0.03	0.03			0.01	0.01	1.9	
L-2-10-14	1024	2077	1023	0.154	1.20	9.8	11.7	10.4	7.9	8.2	7.3	0.43	0.51	0.49	0.13	0.16	0.27	0.34			0.07	0.09	0.08	0.10			0.02	0.02	1.8	
L-2-10-15	1095	2179	1023	0.228	1.33	9.3	12.4	10.4	7.7	8.1	7.4	0.38	0.51	0.49	0.12	0.15	0.25	0.37			0.02	0.03					0.04	0.05	1.9	
L-2-10-16	1192	2501	1023	0.163	1.21	8.5	10.3	10.4	7.7	8.0	7.4	0.46	0.56	0.49	0.14	0.17	0.29	0.38			0.04	0.05					0.03	0.04	1.9	
L-2-10-17	1264	2701	1023	0.193	1.26	9.4	11.9	10.4	8.1	8.6	7.4	0.50	0.64	0.49	0.18	0.23	0.27	0.38			0.04	0.05	0.10	0.13			0.04	0.05	2.0	
L-2-10-18	1360	2977	1023	0.229	1.33	9.5	12.6	10.4	8.2	8.7	7.4	0.41	0.55	0.49	0.12	0.16	0.21	0.33			0.06	0.07	0	0			0.03	0.04	1.9	
L-2-10-19	1432	3153	1022	0.250	1.37	9.8	13.4	10.4	8.3	9.0	7.4	0.60	0.82	0.49	0.10	0.13	0.41	0.58			0.06	0.09	0	0			0.07	0.10	2.0	
L-2-10-20	1528	3407	1022	0.187	1.25	10.6	13.3	10.4	7.7	8.0	7.5	0.43	0.54	0.49	0.07	0.09	0.33	0.48			0.04	0.05	0	0			0.02	0.03	2.0	
L-2-10-21	1600	3565	1022	0.169	1.22	9.9	12.1	10.4	7.9	8.2	7.5	0.32	0.39	0.49	0.14	0.17	0.30	0.43			0.08	0.10	0	0			0.03	0.04	2.0	

[a] Wash water contained Li_2SO_4 at 0.068 *m*.

[b] Dilution factors based on lithium concentration found in sample.

[c] (Reported concentration) × (dilution factor).

[d] Determined from calculated uranium, copper, or sulfate and inventory balance.

[e] Corrected for SO_4^{2-} from Li_2SO_4 and for dilution.

[f] (Reported concentration) × (dilution factor) × (inventory volume).

[g] (Reported concentration corrected for sample dilution and amounts withdrawn in previous samples) × (inventory volume).

[h] Sample taken with reactor down.

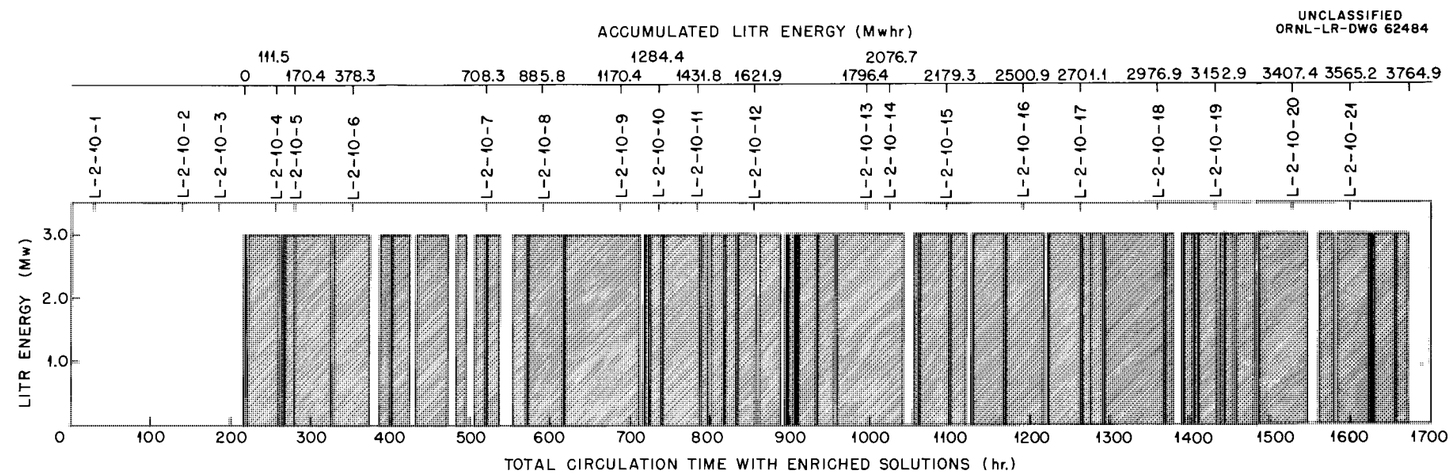

Fig. 4. LITR Operation and Sampling Schedule.

Oxygen partial-pressure measurements were made hourly during the experiment. Radiolytic-gas pressure measurements were made, usually once per week, by measuring the difference in pressure with the reactor in operation just prior to a shutdown and 30 min after the shutdown. Fission and gamma heat measurements were also made at the same time by observing the difference between electric power requirements of the loop heaters during operation at full reactor power and after reactor shutdown. Only one oxygen addition (the original charge) was made during the run. The oxygen partial pressure in the pressurizer, not including the oxygen from radiolytic-gas formation, was 235 psi at the start and decreased during the experiment to a final value of 68 psi.

Two-milliliter samples of solution were taken periodically with the loop at temperature. About 0.2 ml of each sample was used for Cs^{137} analyses. The system was purged with the loop solution before a sample was taken. The volume removed from the circulating stream during the sampling operation was about 11 ml for each sample. The schedule of solution sampling is shown in Table 4 and Fig. 4. Following the original reactor startup, all samples were taken with the reactor at power. Three samples were taken before the reactor went to power.

The experiment was terminated when difficulty with the solution circulation pump was encountered. A sharp increase in pump power requirements produced a "fast setback" and scrammed the reactor. Solution circulation was not completely lost but was decreased to such an extent that the pressurizer temperature started rising and the pressurizer heater power decreased sharply. Following shutdown of the experiment the pump was restarted once, but its operation was still faulty and full circulation could not be restored. The solution was then drained from the loop, and the experiment was removed from the reactor.

Loop areas wetted by the circulating solution are shown in Table 5. In-pile operation of this loop has been reported in detail by Walter.[4]

3.3 Dismantling

The loop was dismantled routinely and without incident. The core, two in-line sample holders, the pressurizer, two sections from the pressurizer heater, a section of piping adjacent to the pump outlet, and the pump were removed from the loop. The remainder of the loop was stored in hole 201 at the burial ground.

Before removal of the pump from the loop the impeller was rotated manually but only with difficulty, evidencing definite binding. The pump was removed from the loop and the volute cut away. Examination of this component and of the impeller revealed no indication of localized attack or presence of foreign material. Further examination showed the rotor end play to be adequate and the rear bearing housing to be pinned securely in place. The bearings had not been mechanically fixed in the housing, however, other than by an interference fit. From the results of subsequent observations and experiments, it has been concluded that failure of the pump probably resulted from failure of the stator windings.[3]

Representative coupons of Zircaloy-2, types 347 and 309 SCb stainless steel from the core channel and annulus arrays, and sections cut from the type 347 stainless steel core body were decontaminated and sent to the Analytical Chemistry Division for induced-activity determinations. These specimens were compared with irradiated control specimens which had been exposed along with standard cobalt samples in the LITR. Two Zircaloy-2 core coupons were also submitted for analysis for hydrogen content.

Table 5. Loop Areas Exposed to High-Temperature Solutions

Components	Stainless Steel Type 347		Stainless Steel 309 SCb		Zircaloy-2		Titanium		Platinum	
	Items	Total Area (cm^2)	Items	Total Area (cm^2)	Items	Total Area (cm^2)	Items	Total Area (cm^2)	Items	Total Area (cm^2)
Loop										
Total main circulation lines (not including pump and core)		1449.5								
Pressurizer (total area 708 cm^2)										
Area wetted when filled with 409 ml of solution		535.0								
Pressurizer lines		243.2								
Core		318.4								
Pump										
Scroll		236.0								
Impeller		214.8								
Specimens and Holders										
24 Core coupons	13	27.3			5	10.5	6	12.6		
2 Clamp bands	2	29.0								
1 CC coupon holder	1	189.8								
3 CA impact specimens					3	71.6				
1 CA spider	1	17.2								
3 CA tensile specimens					3	54.2				
2 CA rods	2	45.4								
20 CA spacers	20	59.0								
18 CA coupled coupons	6	22.8	4	15.2	4	15.2			4	15.2
24 In-line coupons	13	27.3			5	10.5	6	12.6		
2 Clamp bands	2	29.0								
1 In-line coupon holder	1	193.5								
3 In-line impact specimens					3	71.6				
3 In-line tensile specimens					3	54.2				
2 Special line holders	2	26.4								
		3663.6		15.2		287.8		25.2		15.2

Several coupons of each test material from the core and in-line holders, core rod assemblies, and sections from the core cap, pressurizer, pressurizer heater, and main loop piping were sent to the Solid State Division for metallographic examination.[5] The core impact and tensile specimens were not defilmed but were transferred to the Metallurgy group for remote testing.[6]

4. RESULTS AND EVALUATION

4.1 Out-of-Pile

Solution Analyses. – As reported above, two runs with natural-uranium solutions were made during the out-of-pile pretreatment operations. Each pretreatment solution was sampled periodically during loop operation and again following removal from the loop. The samples were analyzed for the constituents originally present in the solutions and for the corrosion products Ni, Fe, Cr, and Al. The pH of each sample was also measured. The results of these analyses are presented in Table 3. The variations in concentrations shown are attributed to analytical errors and/or dilution of the solution in loading the loop or sampling.

The over-all stainless steel corrosion rates, based on the amounts of nickel found in the final solution samples, were 3.0 and 0.4 mpy during the periods of operation with the 0.17 and 0.04 *m* UO_2SO_4 solutions respectively.

Oxygen Consumption Data. – Corrosion rate values, based on oxygen consumption, were calculated with the assumption that all surfaces in contact with high-temperature solution corroded uniformly and that oxygen was consumed by stainless steel only. The oxygen consumption rates were determined by application of measured factors for the relationship between oxygen volume and pressure in the loop. The rates during the periods of operation with 0.17 and 0.04 *m* UO_2SO_4 solutions were 2.8 and 0 mpy respectively.

4.2 In-Pile

Solution Analyses. – Results of solution analyses for constituents other than fission products are shown in Table 4. The first three samples were taken before the reactor went to power and the remainder with the reactor at power.

As for previous loops, Li_2SO_4 was added to the water used to flush the sampling system between removal of samples to provide a means of determining the amount of dilution of the samples by residual flush water in the system.

The reported (i.e., measured), corrected, and calculated values for the uranium, copper, and sulfate concentrations of the samples are compared graphically in Fig. 5. The reported values for uranium were appreciably lower than the calculated values. Correcting the reported values by applying dilution factors based on the amounts of lithium found in the samples resulted in values which were appreciably higher than the calculated concentrations. The reported values for sulfate were all slightly higher than the corresponding calculated values, but since the reported concentrations included those amounts of sulfate associated with the Li_2SO_4 tracer this discrepancy might be expected. However, even after correction for the excess sulfate and for sample dilution, the results remained higher than either the reported or calculated values.

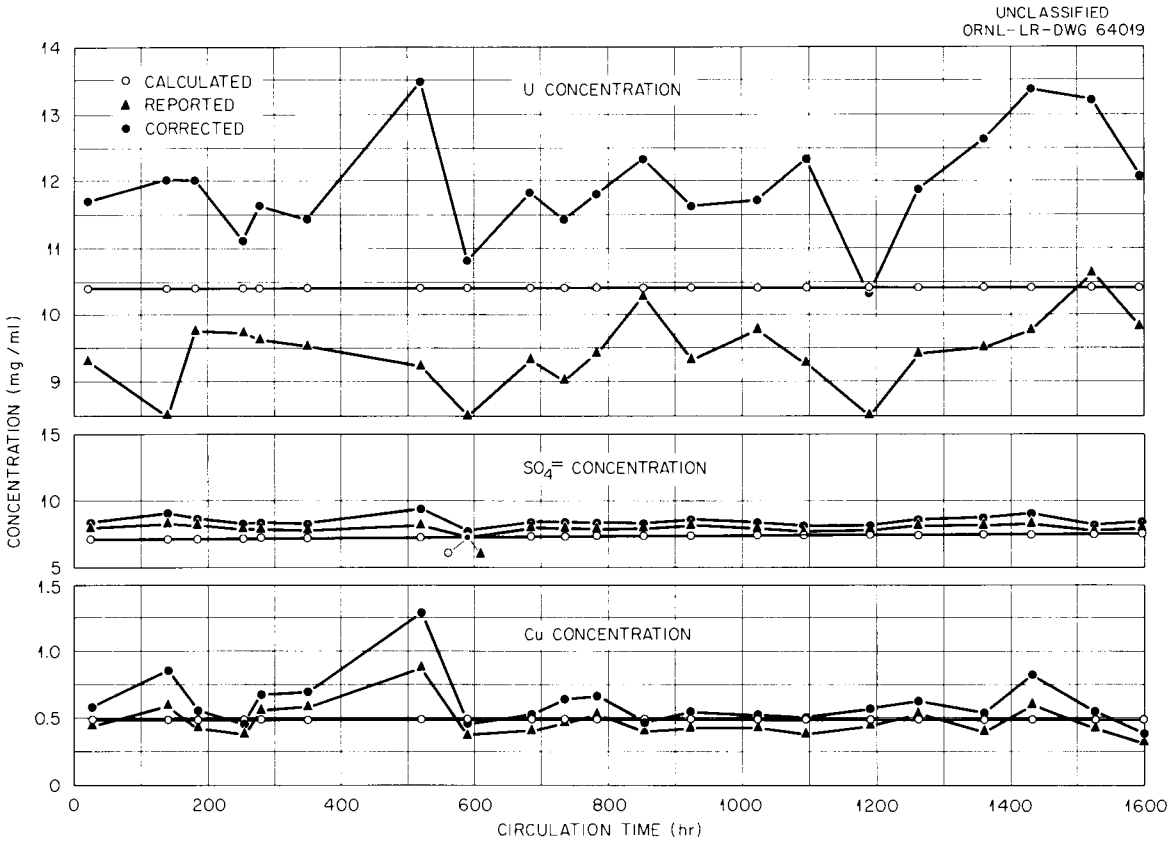

Fig. 5. Comparison of Reported, Corrected, and Calculated Uranium, Sulfate, and Copper Concentrations.

Reported values for the copper concentrations were, in general, slightly lower than the calculated concentrations. Application of dilution factors to these values did not produce corrected values that were in appreciably better agreement with the calculated concentrations.

The nickel and manganese data given in Table 4 are plotted against circulation time in Fig. 6. Also shown on another ordinate in Fig. 6 is the corrosion penetration of type 347 stainless steel, based on both nickel and manganese data. The plot, based on the assumption that all steel surfaces in contact with the high-temperature solution corroded uniformly, indicates an average over-all stainless steel corrosion rate of 0.2 mpy.

The calculated values for corrosion products listed in Table 4, the corrected values for excess H_2SO_4 listed in Table 6 and shown in Fig. 7, and the corrected values for total fissions in Table 10 have been obtained through the use of the listed dilution factors. No correction was applied to pH measurements.

The free sulfuric acid content in the loop solution at the time of each sample withdrawal was calculated on the basis that the H_2SO_4 was neutralized stoichiometrically by the nickel and manganese resulting from corrosion. The amount of nickel, manganese, and the reported, corrected, and calculated free acid in solution at the time of each sample are given in Table 6. Figure 7 is a plot of the nickel and manganese and of the reported, corrected, and calculated values for free acid in solution vs circulation time.

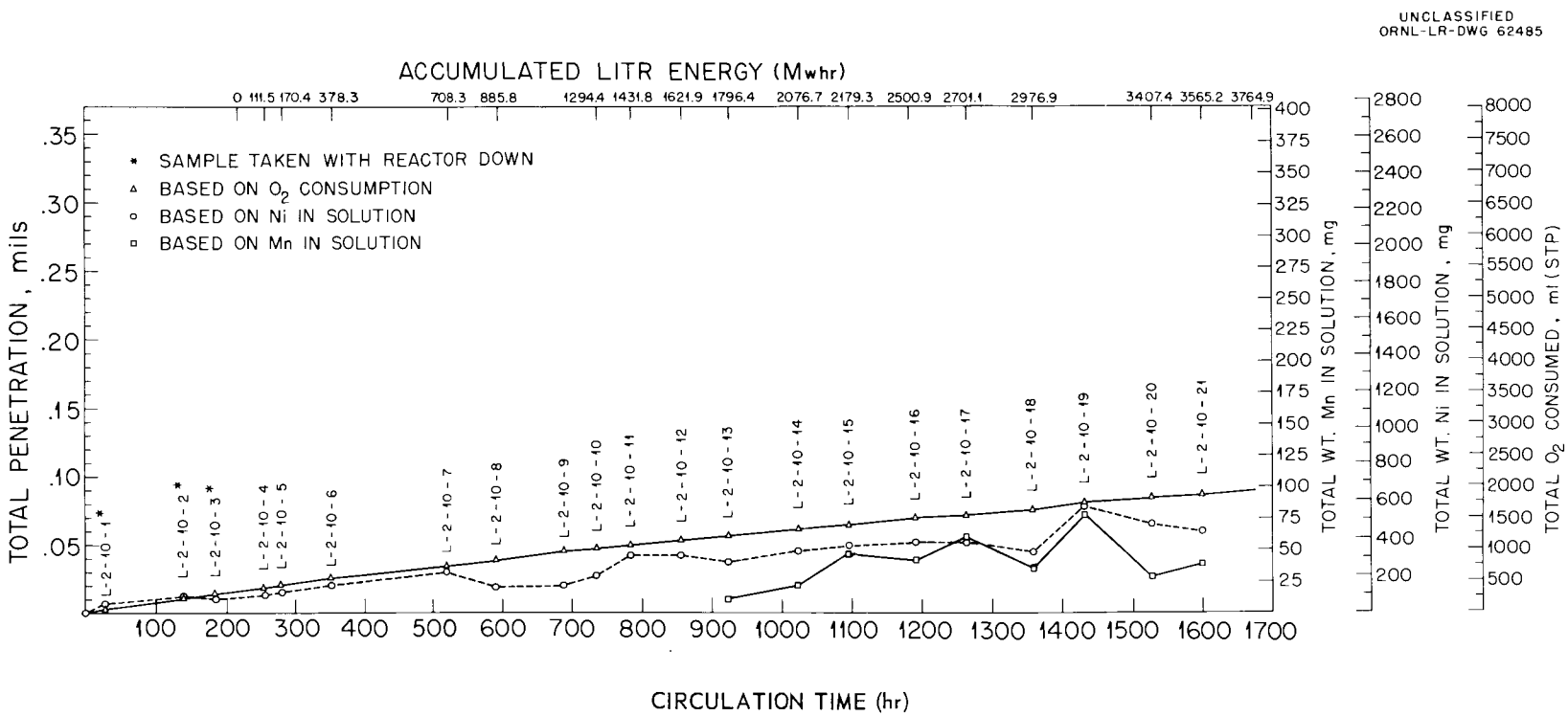

Fig. 6. Over-all Stainless Steel Corrosion Penetration.

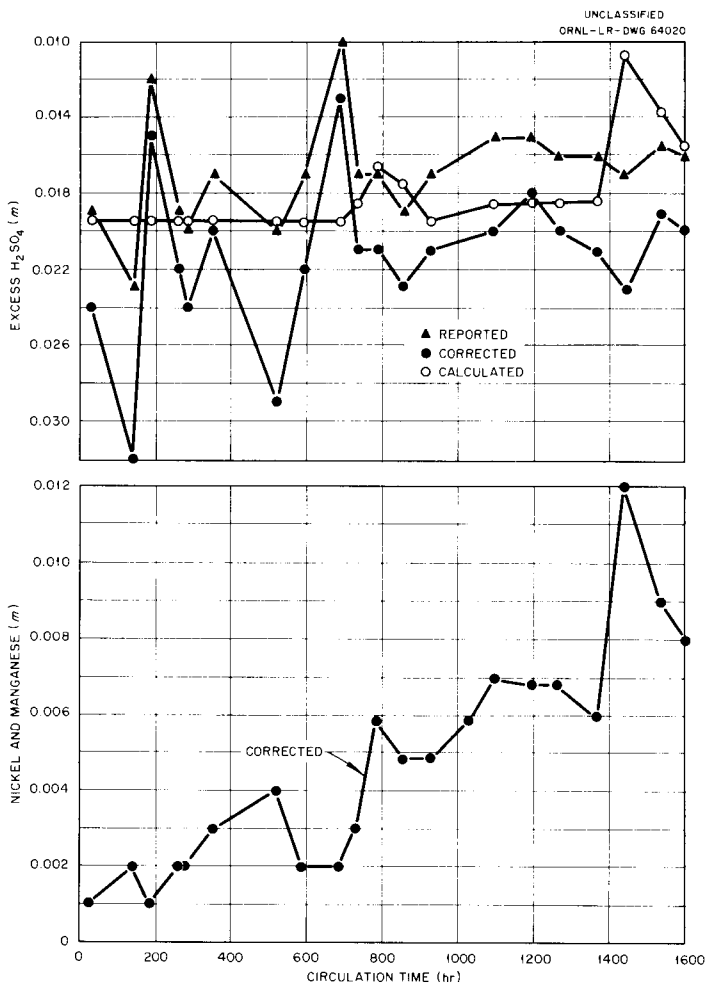

Fig. 7. Nickel plus Manganese and Free Acid in Solution.

The above results indicate that in the present experiment all solution samples were probably diluted before they were withdrawn from the loop sample chamber. The lack of agreement between corrected and calculated concentrations also suggests some error in the tracer technique employed. (The lithium concentrations reported for seven of the samples, L-2-10-2, -7, -15, -18, -19, -20, and -21, appeared unrealistically high.) In addition, sampling and analytical errors cannot be ruled out as possible contributors to the noted lack of agreement in concentrations. Within the experimental uncertainties, no evidence of solution instability was apparent during the period of in-pile operation. It should also be noted that in subsequent experiments, in which revisions to the sampling technique were made to nearly eliminate dilution, more consistent analytical data were obtained.

Oxygen Consumption Data. – Results of oxygen consumption measurements are shown in Table 7. The values for corrosion penetration listed in the final column of Table 7 were calculated with the assumption that all steel surfaces in contact with high-temperature solution corroded uniformly and that oxygen was consumed in the corrosion of steel only. As calculated from the oxygen data, the corrosion rate for the

Table 6. Free H_2SO_4 in Solution

Sample Number	Circulation Time (hr)	Inventory (ml)	Ni and Mn in Solution at Time of Sample[a] (moles)	Free Acid in Solution at Time of Sample		
				Calculated (moles)	Reported (*m*)	Corrected (*m*)
Original charge		1024	0.0		0.021	
L-2-10-1	28	1024	0.001	0.020	0.019	0.024
2	139	1027	0.002	0.020	0.023	0.032
3	184	1024	0.001	0.020	0.012	0.015
4	256	1023	0.002	0.020	0.019	0.022
5	280	1024	0.002	0.020	0.020	0.024
6	352	1024	0.003	0.020	0.017	0.020
7	520	1023	0.004	0.020	0.020	0.029
8	592	1024	0.002	0.020	0.017	0.022
9	688	1023	0.002	0.020	0.010	0.013
10	736	1023	0.003	0.019	0.017	0.021
11	784	1023	0.006	0.017	0.017	0.021
12	855	1023	0.005	0.018	0.019	0.023
13	924	1023	0.005	0.019	0.017	0.021
14	1024	1023	0.006	0.018		
15	1095	1023	0.007	0.017	0.015	0.020
16	1192	1023	0.007	0.017	0.015	0.018
17	1264	1023	0.007	0.017	0.016	0.020
18	1360	1023	0.006	0.017	0.016	0.021
19	1432	1022	0.012	0.011	0.017	0.023
20	1528	1022	0.009	0.014	0.015	0.019
21	1600	1022	0.008	0.016	0.016	0.020

[a]Includes amounts previously withdrawn in samples.

entire operation was about 0.4 mpy. Unlike previous experiments employing steel core bodies, no initial high corrosion rate was observed in this experiment. Oxygen was consumed at a steady rate throughout the period of in-pile operation. A plot of oxygen consumption vs circulation time is shown in Fig. 6.

Since, however, some of the oxygen must have been consumed by materials other than stainless steel, the over-all stainless steel rate of 0.4 mpy is high. As shown in Table 3, only about 90% of the wetted loop surface was stainless steel. An approximate correction for the amount of oxygen consumed by other materials, based on the measured weight losses of the corrosion specimens in the loop, resulted in a reduction in stainless steel rates of about 10%. Employing the corrected oxygen volumes, the over-all stainless steel rate for the period of operation was about 0.35 mpy. As reported above, the over-all stainless steel corrosion rate, based on the amounts of nickel and manganese found in solution, was about 0.2 mpy.

Table 7. Oxygen Consumption in Loop[a]

Sample Number	LITR Energy (Mwhr)	Total Solution Circulation Time (hr)	O_2 Additions to Loop (cc at STP)	O_2 Withdrawn from Loop[b] (cc at STP)	Total O_2 Charged to Loop Less O_2 Withdrawn in Sampling (cc at STP)	O_2 Volume at Time of Sample (cc at STP)	O_2 Consumed Since Last Sample (cc at STP)	Total O_2 Consumed (cc at STP)	Calculated Corrosion Penetration of Type 347 Stainless Steel (mils)
(L-2-10-8)[c]	0	0	3020	0	3020	3020	0	0	0
L-2-10-1	0	28	0	18	3002	2926	76	76	<0.01
L-2-10-2	0	139	0	16	2986	2738	172	248	0.01
L-2-10-3	0	184	0	16	2970	2643	79	327	0.02
L-2-10-4	111	256	0	15	2955	2572	56	383	0.02
L-2-10-5	170	280	0	15	2940	2508	49	432	0.02
L-2-10-6	378	352	0	14	2926	2375	119	551	0.03
L-2-10-7	708	520	0	13	2913	2172	190	741	0.03
L-2-10-8	886	592	0	12	2901	2068	93	834	0.04
L-2-10-9	1170	688	0	11	2890	1907	149	983	0.05
L-2-10-10	1294	736	0	11	2878	1851	44	1027	0.05
L-2-10-11	1432	784	0	11	2868	1798	43	1070	0.05
L-2-10-12	1622	855	0	10	2858	1715	74	1144	0.05
L-2-10-13	1796	924	0	10	2849	1634	71	1215	0.06
L-2-10-14	2077	1024	0	9	2840	1513	112	1327	0.06
L-2-10-15	2179	1095	0	9	2831	1448	56	1383	0.06
L-2-10-16	2501	1192	0	8	2823	1327	113	1496	0.07
L-2-10-17	2701	1264	0	7	2816	1263	56	1553	0.07
L-2-10-18	2977	1360	0	7	2809	1164	90	1643	0.08
L-2-10-19	3153	1432	0	6	2803	1071	89	1732	0.08
L-2-10-20	3407	1528	0	6	2797	991	74	1806	0.08
L-2-10-21	3565	1600	0	6	2791	933	53	1859	0.09
Pump off, solution drained	3765	1672	0	0	2791	869	64	1922	0.09

[a]The average quantity of oxygen in the loop, at a given partial pressure of oxygen, was 12.8 cc (STP)/psi.
[b]Calculated amount removed as O_2 dissolved in sample.
[c]Oxygen addition.

Uranium Balance. – The balance sheet for the uranium charged to and recovered from the loop experiment is shown in Table 8. The weigh-tank contents, consisting of the entire solution volume circulated in the loop (except for amounts removed as samples), enriched make-up solution remaining in the fuel reservoir upon termination of the experiment, and water used to rinse the loop after removal of the UO_2SO_4 charge, were emptied at the end of operation. Analytical results indicate that 1.6% less uranium was recovered than was charged to the experiment.

Neutron Flux, Fission Power, and Gamma Heat. – *Results.* – The thermal-neutron flux at a given position in the core was determined from induced-activity measurements of representative Zircaloy-2 and type 347 stainless steel coupons from the core channel and core annulus coupon arrays, and from type 309 SCb stainless steel core annulus coupons. In addition, measurements were made of ten of the type 347 stainless steel core annulus coupon spacers and of three pieces cut from the wall of the type 347 stainless steel core body. The specimens were decontaminated prior to counting. The Zr^{95}-Nb^{95} activity was employed for the Zircaloy-2 determinations and the Cr^{51} activity for the stainless steel specimens. The results are given in Table 9. In Fig. 8, the logarithms of the neutron fluxes of the specimens are plotted

Table 8. Uranium Balance

Source	Solution Weight (g)	Specific Gravity	Solution Volume (ml)	U Conc. by Analysis (mg/ml)	Uranium Weight (92.66% U^{235}) (g)
		Charged to Loop			
Original solution charged to loop	1041.3	1.017[a]	1023.9[b]	10.4[a]	10.7[b]
Make-up solution charged to loop (including fuel from reservoir)	580.9[b]	1.017[a]	571.2	10.4[a]	5.9
				Total	16.6
		Recovered from Loop			
Loop inventory samples to laboratory	34.8[b]	1.017[c]	34.2	8.5–10.6	0.3
Weigh-tank samples to laboratory	15.3[c]	1.0[c]	15.3	0.5–2.4	0.02
Weigh-tank contents (including fuel from reservoir)	11,500[c]	1.0[a]	11,500[c]	1.4[d]	16.0
				Total	16.3

Material balance = –1.6%.

[a]Average from analyses.
[b]Calculated.
[c]Assumed.
[d]Weigh-tank reading.

Table 9. Induced Activity in Zircaloy-2 and Types 347 and 309 SCb Stainless Steel Specimens

Specimen Number	Cleaned Weight When Counted (g)	Relative Zr^{95}-Nb^{95} Activity	Relative Cr^{51} Activity	Specimen Exposure Time: Total (hr)	Specimen Exposure Time: Equivalent Time at 3 Mw (Mwhr/3 Mw)	Cooling Time Before Analysis (hr)	Neutron Flux at 3 Mw (neutrons cm^{-2} sec^{-1})	Power Density at 3 Mw (w/ml)	Distance from Leading Edge of First Core Channel Coupon (in.)
							$\times 10^{12}$		
Zircaloy-2									
Core Channel Coupons									
Z-83	0.5337	7.22		1457	1255	3312	4.7	1.6	3.6
Z-80	0.4364	14.50		1457	1255	3312	9.5	3.2	1.9
Core Annulus Coupons									
Z-99	0.7205	1.67		1457	1255	3288	7.2	2.5	3.2
Z-96	0.7118	2.03		1457	1255	3288	8.7	3.0	2.5
Type 347 Stainless Steel									
Core Channel Coupons									
1138A	0.7737		6.18	1457	1255	1968	12.3	4.2	0.1
1247A	0.7543		5.43	1457	1255	1968	10.7	3.7	0.6
1255A	0.7814		4.66	1457	1255	1968	9.2	3.2	1.1
1374A	0.8163		2.48	1457	1255	1968	4.9	1.7	3.1
1379A	0.6486		1.38	1457	1255	1968	2.8	1.0	5.1
1382A	0.6801		1.20	1457	1255	1968	2.3	0.8	5.9
Core Annulus Coupons									
961-A	0.3817		1.11	1457	1255	2304	10.5	3.6	1.4
966-A	0.3876		0.76	1457	1255	2304	7.2	2.5	3.9
Core Annulus Spacers									
1	0.4229		10.5	1457	1255	2424	11.5	4.0	1.2
2	0.4410		10.7	1457	1255	2424	11.7	4.0	1.6
3	0.4979		7.02	1457	1255	2424	7.7	2.7	2.0
4	0.4475		8.19	1457	1255	2424	9.0	3.1	2.3
5	0.5225		5.81	1457	1255	2424	6.4	2.2	2.7
6	0.4436		7.33	1457	1255	2424	8.0	2.8	3.0
7	0.4915		7.21	1457	1255	2424	7.9	2.7	3.4
8	0.4124		4.90	1457	1255	2424	5.4	1.9	3.8
9	0.4980		5.44	1457	1255	2424	6.0	2.1	4.1
10	0.4859		4.17	1457	1255	2424	4.6	1.6	4.5
Core Body Wall									
B	1.2753		17.1	1457	1255	2424	18.5	6.5	−1.0
C	1.8138		11.4	1457	1255	2424	12.5	4.4	0.6
D	0.8790		4.61	1457	1255	2424	5.0	1.8	4.8
Type 309 SCb Stainless Steel									
Core Annulus Coupons									
C-2	1.4940		0.67	1457	1255	2304	6.4	2.2	3.2
C-3	1.5306		0.77	1457	1255	2304	7.3	2.5	2.5
Control Specimens									
Zircaloy-2									
W-118	0.7826	1.0		50.0		3144	12.2		
W-119 (A + B)	1.5899	1.0		105.6		2928	42.0		
Type 347 Stainless Steel									
1134-A (W-211)	0.9526		1.0	50.0		1800	12.2		
W-212-A	1.0451		1.0	105.6		1944	42.0		
Type 309 SCb Stainless Steel									
W-302-B	0.9105		1.0	105.6		1944	42.0		

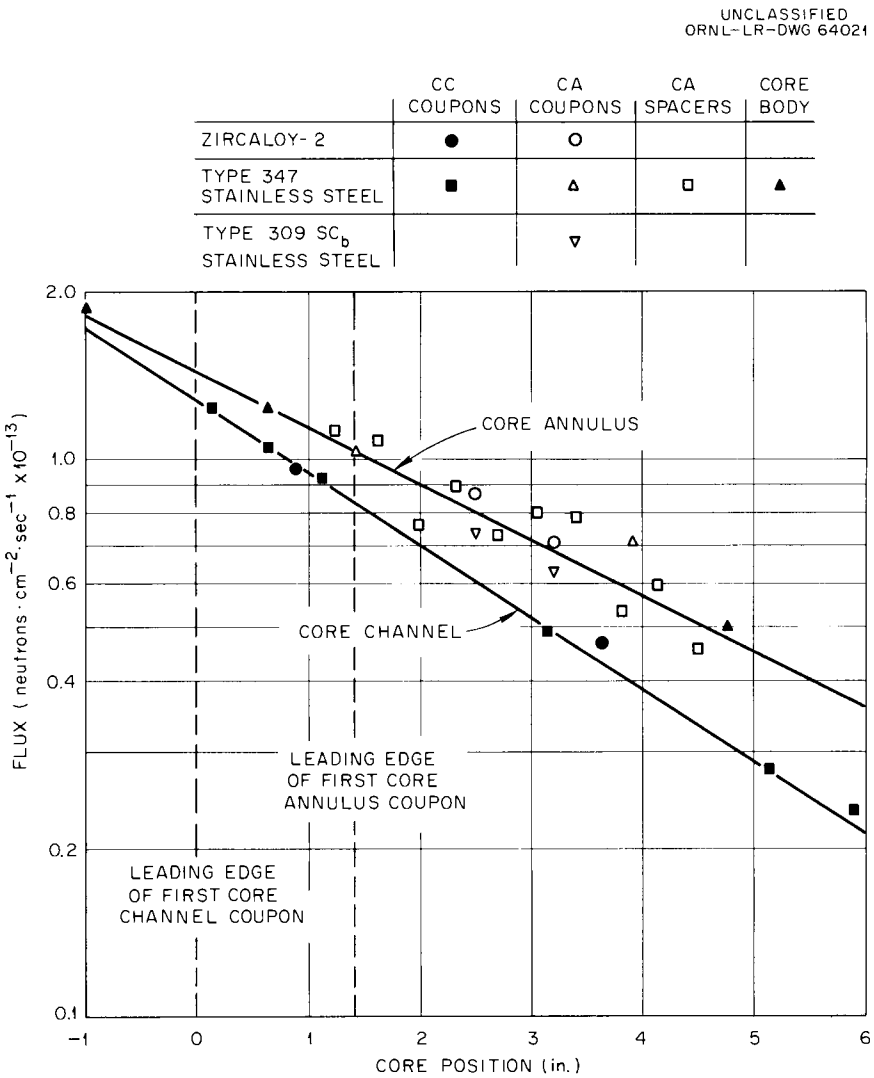

Fig. 8. Flux in Core.

against the positions of the specimens. The two lines shown were obtained from least-squares analyses of thermal-neutron flux data for stainless steel and Zircaloy-2 core coupons at various positions and for stainless steel and Zircaloy-2 core rod coupons and stainless steel spacers. As shown, the flux in the core channel position ranged from 12.3×10^{12} thermal neutrons cm^{-2} sec^{-1} at the position of the leading core channel coupon (0.13 in.) to 2.3×10^{12} at the position of the rear core channel coupon (5.9 in.). The flux values in the core annulus were observed to be greater than for the equivalent core channel positions and ranged from 10.5×10^{12} neutrons cm^{-2} sec^{-1} at the position of the leading annulus coupons (1.4 in.) to 5.4×10^{12} at the rear of the core annulus arrays (4.3 in.). The thermal flux at the nose of the core, located about 1.4 in. from the reactor lattice, was about 1.7 to 1.8×10^{13}.

The solution fission power densities at the specimen positions were calculated by using the thermal-neutron fluxes thus determined. The power densities, based on a value of 200 Mev for the average energy

per fission, ranged from 4.2 w/ml for the foremost core channel coupon to 0.8 w/ml for the rear core channel coupon; corresponding values for the core annulus coupons ranged from 3.6 to 1.9 w/ml. From the logarithmic-mean averages of the solution power densities in the core channel and annulus positions, an average power density of 2.8 w/ml was obtained for the core solution.

During full-power operation the average fission power of the loop, obtained from beta-spectrometer analyses for Cs^{137} and a value of 200 Mev/fission, was 492 w. Results of the analyses are given in Table 10, and represent the average power between samples. The average power in the core, based on these results, was about 1.7 w/ml.

Table 10. Fissions in Loop Solution[a]

Sample Number	Accumulated LITR Energy (Mwhr)	Inventory Volume at Time of Sample (ml at 25°C)	Calculated Uranium Concentration (mg/ml)	Total Fissions per Milliliter		Total Fission Power in Loop Solution at 3 Mw (w)
				Analysis	Corrected[b]	
				$\times 10^{15}$	$\times 10^{15}$	
L-2-10-1	0.0	1023.9	10.4			
-2	0.0	1026.7	10.4			
-3	0.0	1023.7	10.4			
-4	111.5	1023.4	10.4	1.61	1.85	452
-5	170.4	1023.8	10.4	2.60	3.15	504
-6	378.3	1023.9	10.4	5.41	6.53	471
-7	708.3	1023.4	10.4	11.3	16.6	638
-8	885.8	1024.3	10.4	9.31	12.2	376
-9	1170.4	1023.4	10.4	14.7	19.0	506
-10	1294.4	1023.3	10.4	17.0	22.1	465
-11	1431.8	1023.2	10.4	20.1	26.1	497
-12	1621.9	1022.8	10.4	24.7	30.7	515
-13	1796.4	1023.4	10.4	26.3	34.3	520
-14	2076.7	1023.3	10.4	28.8	36.3	476
-15	2179.3	1023.3	10.4	28.8	40.5	507
-16	2500.9	1023.3	10.4	32.6	42.0	458
-17	2701.1	1022.9	10.4	32.6	44.1	445
-18	2976.9	1023.4	10.4	36.4	51.7	472
-19	3152.9	1022.2	10.4	40.0	58.7	506
-20	3407.4	1022.3	10.4	44.9	60.7	484
-21	3565.2	1022.2	10.4	56.5	74.1	566
		Av 1023.4				492

[a]Calculated on basis of 200 Mev/fission.

[b]Corrected to include amounts withdrawn in previous samples and for sample dilution.

The average combined fission and gamma heat at 3 Mw reactor power, as determined from the difference in electric-heater power requirements with the reactor down and at full power, was 1256 w. As shown in Fig. 9, there was no significant drift or shift of values during the run. The three curves in Fig. 9 represent the wattage required when the reactor was operating, that required when the reactor was not operating, and the wattage equivalent to the difference of the two curves. If, as reported for subsequent stainless steel loops operated in the HB-2 beam hole,[7] an average value of 700 w for the gamma component is assumed, the heat in the core solution resulting from the fission component was about 1.9 w/ml.

Evaluation. – As shown in Fig. 8, the calculated values for thermal-neutron fluxes in the core of this experiment, based on both the steel and Zircaloy-2 measurements, indicated not only the usual axial gradient but also a radial gradient. The average thermal-neutron flux in the core annulus appears to have been about 25% greater than that for the specimens inside the core channel holder. This was the first experiment in which a radial gradient has been observed. Since this was the first experiment to employ type 347 stainless steel core channel coupon holders (all previous holders were Zircaloy-2 or titanium), it is possible that the high neutron-capture cross section of the steel shielded the core channel coupons sufficiently to produce this result. Indeed, results from subsequent experiments that employed Zircaloy-2 core channel holders and were operated in the HB-2 beam hole did not indicate radial gradients. The thermal-neutron flux pattern in both the core channel and core annulus regions of this experiment are compared in Fig. 10 with the thermal-flux values as determined in the previous HB-4 experiments.

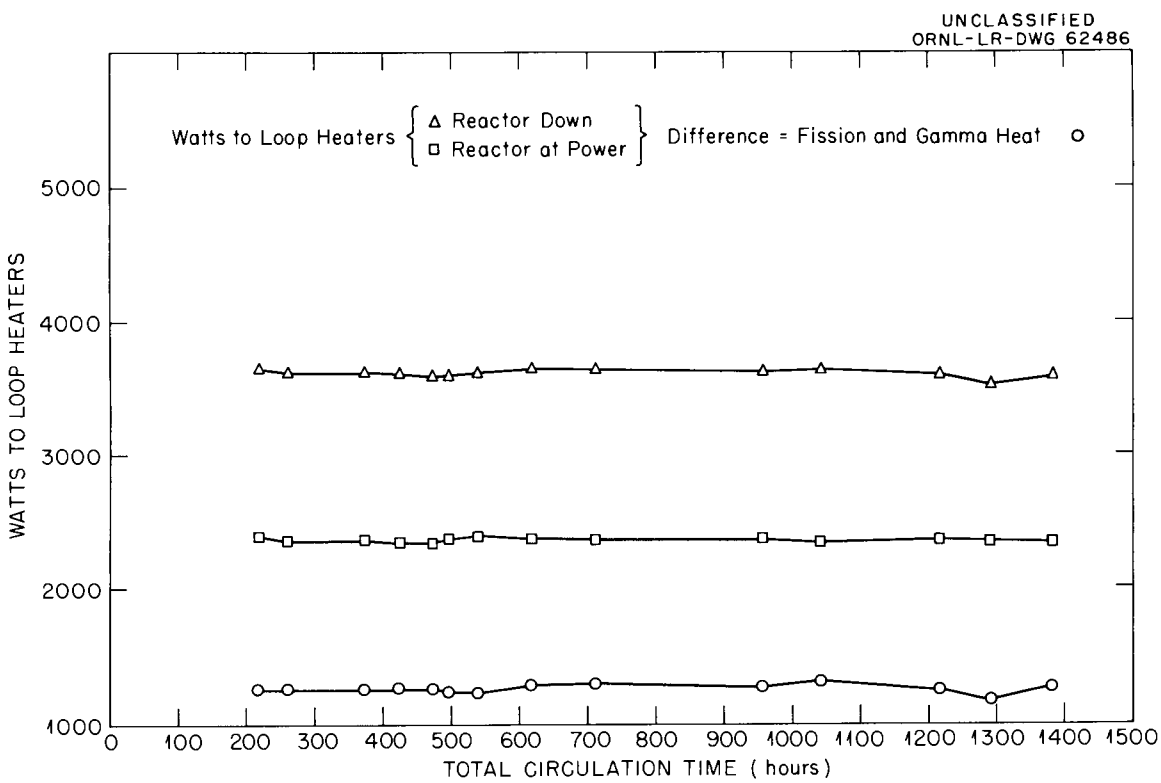

Fig. 9. Power to Loop Heaters and Fission and Gamma Heat.

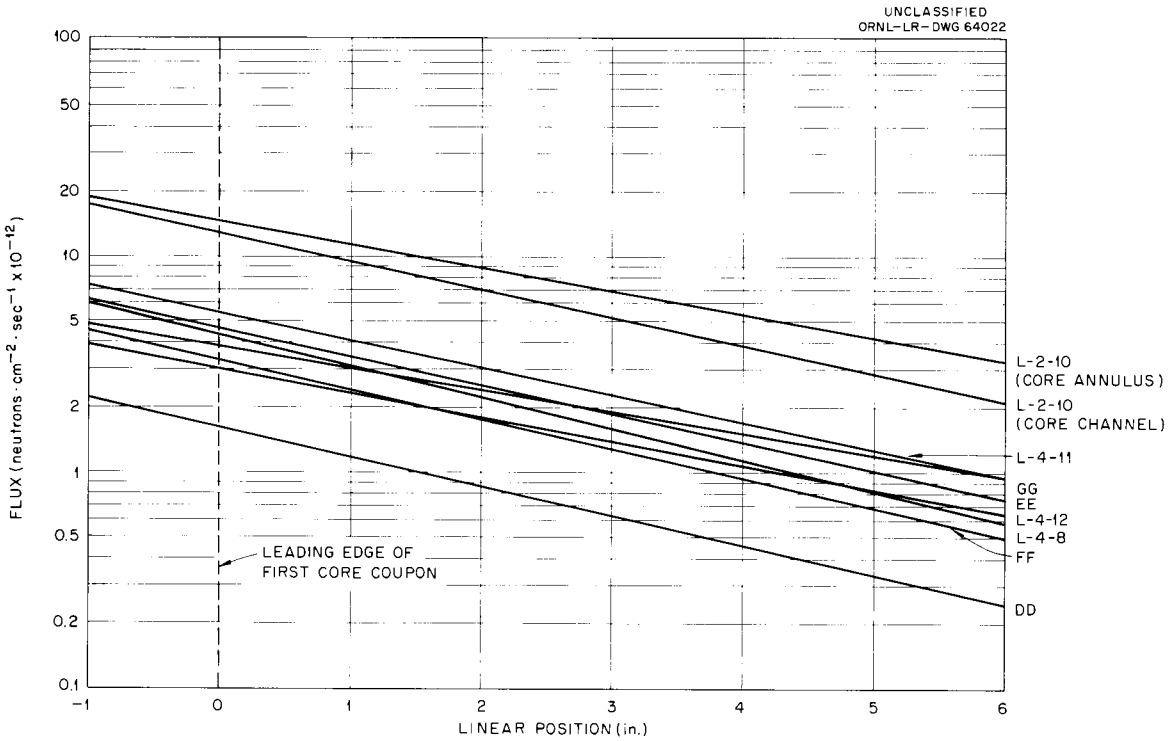

Fig. 10. Flux in Core vs Axial Position.

As reported above, the estimated average fission power in the core of this experiment was about 2.8 w/ml based on specimen-activity measurements and only 1.7 w/ml based on Cs^{137} analyses. The value of 1.9 w/ml for the average fission power determined from measurements of the combined fission and gamma heat represents only the fission energy absorbed within the loop. This has been estimated at about 170 Mev/fission. When the power values determined from Cs^{137} and from the Zr^{95}-Nb^{95} and Cr^{51} activity measurements are compared on a basis of 170 Mev/fission instead of the 200 Mev/fission employed above, they are about 1.5 and 2.4 w/ml respectively. The discrepancy between the activity and fission-heat results may be associated with an error in the flux values determined from the Zr^{95}-Nb^{95} and Cr^{51} induced-activity measurements. The inclusion of cobalt flux monitors in experiments operated in the same reactor beam hole, subsequent to the present experiment, has shown that the thermal flux based on Zr^{95}-Nb^{95} activity may be as much as 30% greater than that based on Co^{60}. Application of this possible correction to the 2.4-w/ml value from the activity measurements results in an average solution fission-power-density value of 1.9 w/ml. It appears likely that the Cs^{137} results are in error, but the explanation for this is not apparent.

Radiolytic-Gas Pressure. – The average radiolytic-gas pressure in the pressurizer at 3-Mw reactor operation was 6.1 ± 0.5 psi as determined by special pressure-temperature measurements before and after reactor shutdowns, and 6.8 ± 0.4 psi as determined from the partial-pressure plot. There was no statistically significant drift or change in radiolytic-gas pressure during the run. The calculated molar rate con-

stant for copper, used in the solution as a catalyst for the recombination of radiolytic gas formed during loop operation at power, was 10,900 hr^{-1} $mole^{-1}$ $liter^{-1}$ (volume at STP) at 280°C, based on an activation energy for copper of 25 kcal/mole.[8]

4.3 Qualitative Inspection of Loop

All component surfaces outside the core region were covered with a heavy black rustlike scale. The scale was darker than that found in similar locations in previous loops. Figure 11, a view of the in-line Zircaloy-2 impact and tensile specimens and the specimen holder in the "as-removed" condition, and Fig. 12, a view of the "as-removed" in-line coupon holder and specimen array, show the uniform appearance of

UNCLASSIFIED
PHOTO 18620

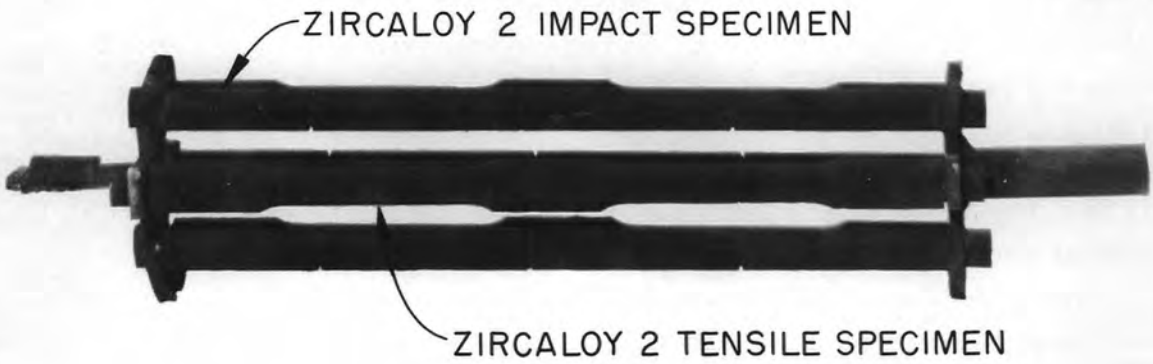

Fig. 11. Special In-Line Assembly.

UNCLASSIFIED
PHOTO 18714

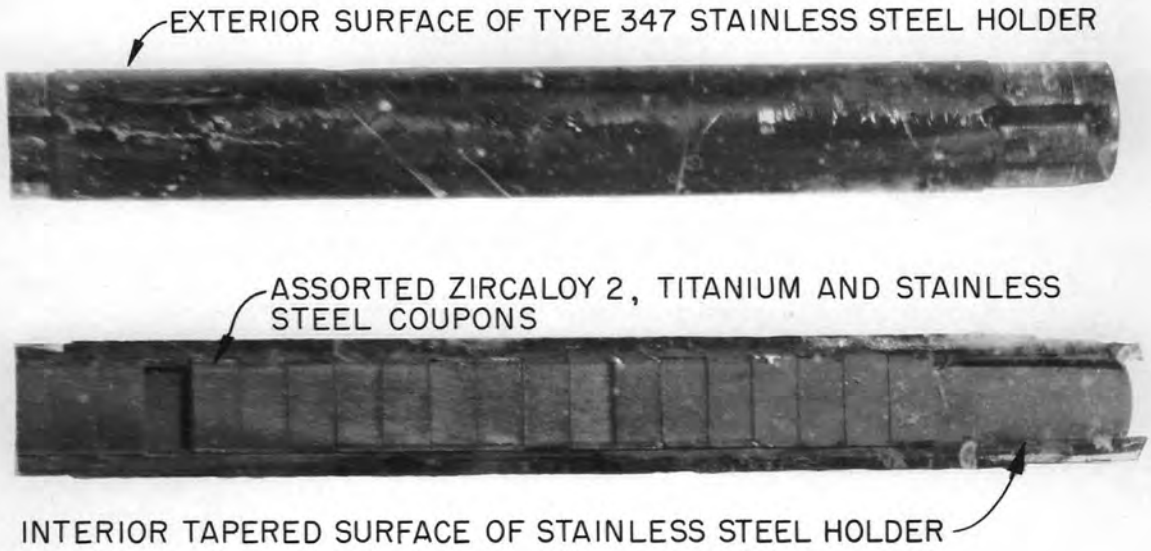

Fig. 12. In-Line Coupon Array.

the scale on all surfaces, irrespective of material. A similar scale was found on the pressurizer wall; however, in this case, the deposit in the liquid-phase region was heavier than that found in the vapor-phase region. In addition, the scale in the vapor-phase region had a gray hue.

Unlike previous loops, the stainless steel surfaces in the core region were not covered with the usual black scale. In Fig. 13, a view of the "as-removed" core specimen assembly, and Fig. 14, a view of the "as-removed" core holder and coupon array, it may be seen that the type 347 stainless steel core coupon holder was almost free of bulk scale on the forward or high-flux end, but gradually acquired a black velvety scale from approximately the midpoint to the rear of the holder. The same graduation of scale thickness may be observed on the type 347 stainless steel core coupons. The scale deposit on the inside of most of the type 347 stainless steel core body ranged from rust red in appearance at the high-flux end to a heavy black-appearing deposit at the low-flux end. This scale also showed several spots of discoloration in areas adjacent to the rod coupons contained in rod assembly A. (Rod A was located at a position 30° below horizontal, and rod B was 30° above horizontal in the core annulus. Rod A was also located much closer to the core-body wall than was Rod B). Figure 15 is a photograph of the interior of the core. The relative locations of the core rod coupons to the areas of discoloration are also shown. The local discolorations can be correlated with the adjacent rod A coupons as follows:

1. In regions adjacent to the stainless steel coupons the scale was heavy and was dull gray in color.
2. Scale in regions adjacent to Zircaloy-2 coupons was heavy and black.
3. Areas adjacent to platinum coupons were generally rust-red in color with the scale becoming thinner toward the center of the discolored area. In the center of each area was located a thin, black band of scale approximately $\frac{1}{16}$ in. wide.
4. A noticeable rust-red spot of film was found on the core nose opposite the end of the rod A assembly.

UNCLASSIFIED
PHOTO 18645

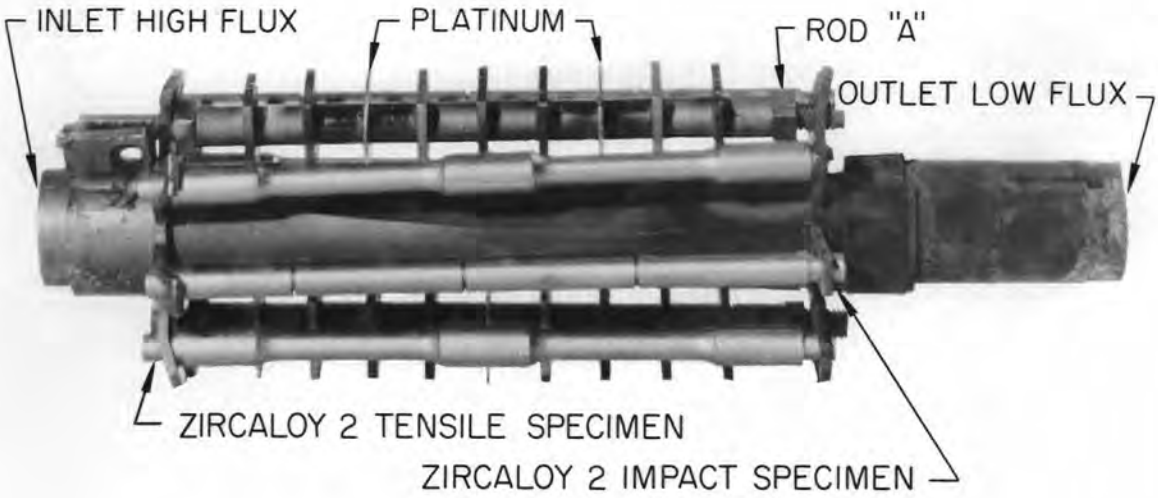

Fig. 13. Core Specimen Assembly.

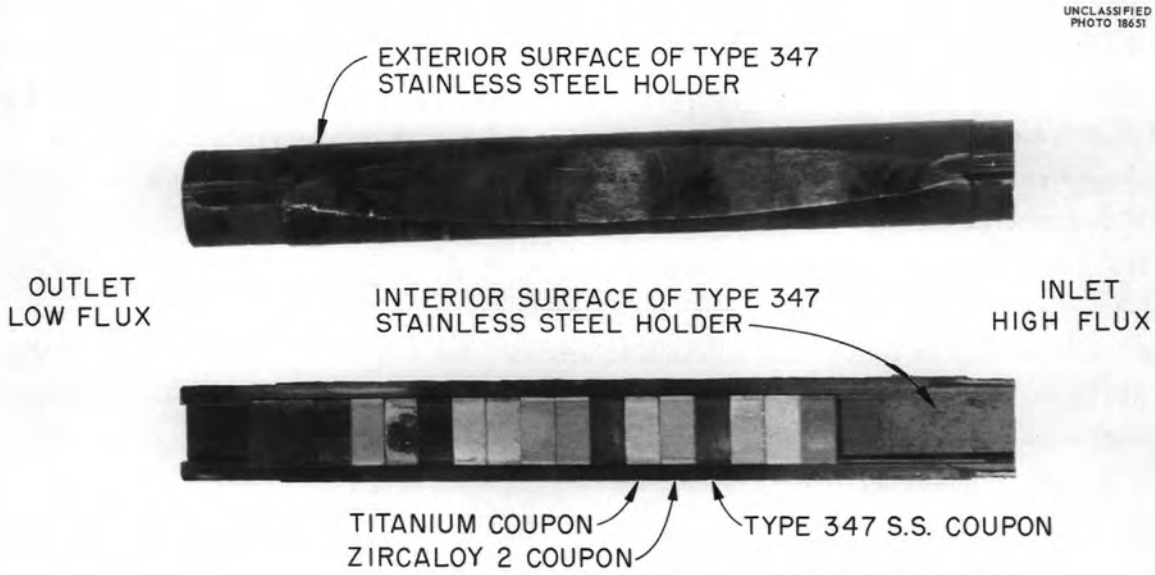

Fig. 14. Core Coupon Array.

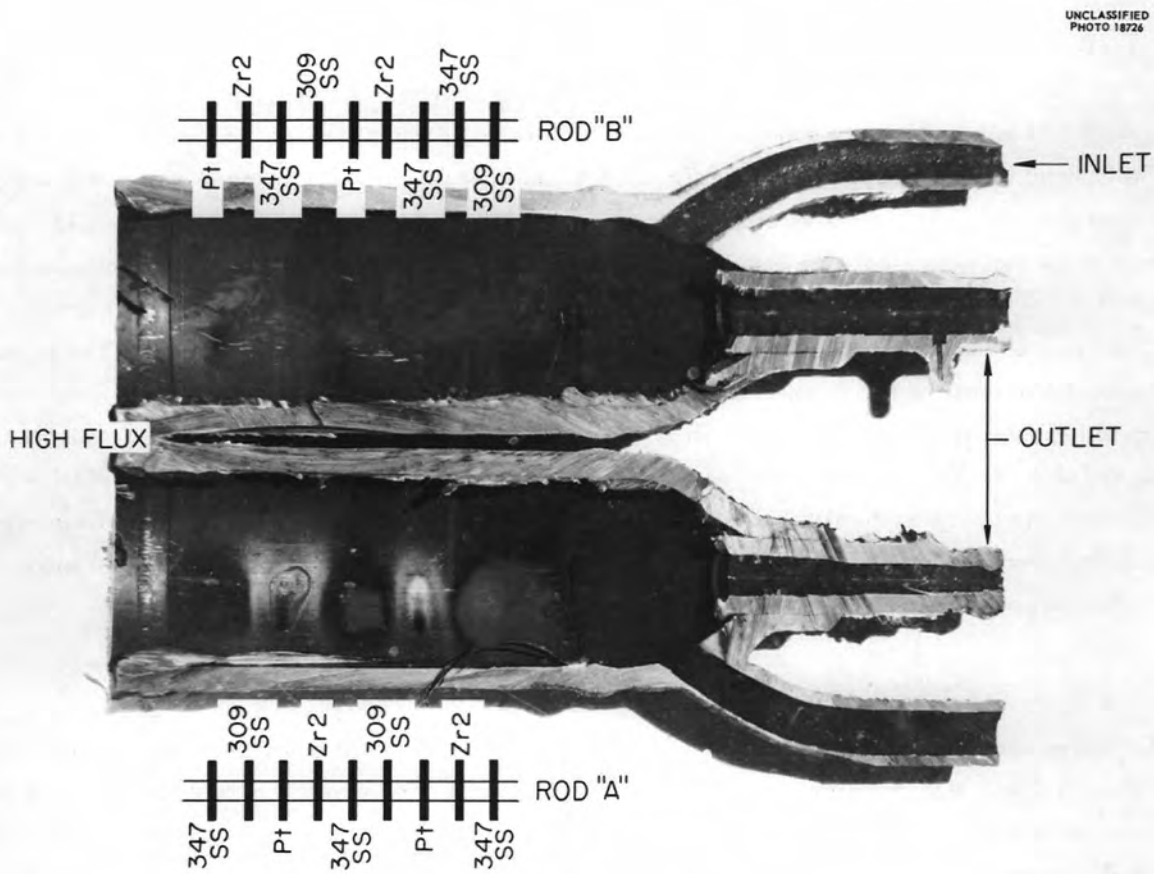

Fig. 15. Loop Core.

The two core rod assemblies differed in their "as-removed" appearance. Rod B assembly was covered with a rustlike scale, becoming heavier toward the low-flux end. Rod A assembly had a very much thinner scale deposit, particularly in the high-flux regions. In addition, as can be seen in Fig. 13, four of the stainless steel spacers (adjacent to both platinum coupons on rod A) were covered with a thin iridescent film. This same type of film was subsequently noted on the Zircaloy-2 impact specimens located in the loop L-2-14 core annulus.[7]

The Zircaloy-2 and titanium core coupons had only slight amounts of scale deposit, the coupons located in the high-flux regions having practically none.

As with previous loops the standard cathodic defilming was only partially effective; some film was retained by the specimens after this treatment. All Zircaloy-2 in-line coupons showed weight increases or no weight change following the final defilming.

Individual qualitative descriptions of the specimens contained in this experiment are given in Table 11.

4.4 Metallographic Examinations

Metallographic findings for this loop have been previously reported by Stiegler.[5] A summary of his findings including quotations from his report are given here.

"There was no evidence of extensive attack on the type 347 stainless steel sections from the pressurizer heater inlet and outlet or the main loop piping near the pump outlet. However, both the inlet and outlet sections of the pressurizer heater showed some slight penetration at the grain boundaries to a maximum depth of 1 mil, and a crack approximately 5 mils deep was noted at the intersection between the base and weld metal of the pump outlet piping. This crack can most likely be attributed to incomplete fusion during welding and not to corrosive attack." A photomicrograph of this crack is shown in Fig. 16. "The surface of the stainless steel core cap was rough and uneven but there was no evidence of intergranular attack."

Corrosion estimates from thickness measurements and metallographic observations of the corrosian coupons were in reasonable agreement with the weight loss data. A summary of dimensional measurements and metallographic results from examination of a large group of corrosion coupons from this experiment is given in Table 12. "The attack on types 347 and 309 SCb stainless steel coupons was of a shallow pitting nature while the attack on the titanium-55A and Zircaloy-2 coupons was of a more generalized surface-roughening nature. The thickness of all the coupons examined remained essentially constant along their entire lengths, neither increasing nor decreasing notably in the clamping regions."

4.5 Quantitative Inspection of Loop

Corrosion-Specimen Weight Data. – Sample weight data, together with other pertinent information, are presented in Table 11. Two different values for corrosion penetration were calculated for each specimen from the weight-change data. One value is based on the exposed area of the specimen, and the other is based on the total area. Two different corrosion-rate values are listed for each penetration value. One was computed with total circulation time as a basis; the other with radiation time as a basis. The value for the

Table 11. Data for Corrosion Specimens

Sample Number	Position	Av Flow Velocity Across Specimen (fps)	Weight Data: Initial (g)	Weight Data: As Removed (g)	Weight Data: Defilmed (g)	Weight Data: Change (mg)	Exposed Sample Area (cm^2)	Corrosion Penetration (mils)	Corrosion Rate[a] (Exposed Area) (mpy): 1672 hr	Corrosion Rate[a] (Exposed Area) (mpy): 1255 hr	Corrosion Penetration (mils)	Corrosion Rate[a] (Total Area) (mpy): 1672 hr	Corrosion Rate[a] (Total Area) (mpy): 1255 hr	Distance from Front of First Specimen to Center of Specimen (in.)	Neutron Flux at Specimen Locations (neutrons/cm^2/sec × 10^{-12})	Power Density at Specimen Locations (w/ml)	As Removed	Defilmed
24 Core Corrosion Sample Coupons (total area each, 2.1 cm^2)																		
Stainless Steel Type 347																		
1138A	1	8.9	0.9632	0.9509	0.9503	12.9	1.57	0.41	2.1	2.8	0.30	1.6	2.1	0.13	12.28	4.2	Thin dark scale over all surfaces	Some stain retained; machine marks visible
1245A	2	9.5	0.9506	0.9414	0.9413	9.3	1.40	0.33	1.7	2.3	0.22	1.2	1.5	0.38	11.50	3.9	Thin dark scale over all surfaces	Some stain retained; machine marks visible
1247A	3	10.4	0.9531	0.9456	0.9450	8.1	1.40	0.29	1.5	2.0	0.19	1.0	1.3	0.63	10.74	3.7	Thin dark scale over all surfaces	Some stain retained; machine marks visible
1251A	4	11.4	0.9471	0.9405	0.9407	6.4	1.40	0.23	1.2	1.6	0.15	0.8	1.1	0.88	9.90	3.4	Thin dark scale over all surfaces	Some stain retained; machine marks visible
1255A	5	12.7	0.9611	0.9557	0.9558	5.3	1.40	0.19	1.0	1.3	0.12	0.7	0.9	1.13	9.21	3.2	Thin dark scale over all surfaces	Clean; machine marks clearly visible
1372A	7	16.0	0.9605	0.9577	0.9569	3.6	1.40	0.13	0.7	0.9	0.09	0.5	0.6	1.63	7.90	2.7	Thin dark scale over all surfaces	Some stain retained; machine marks visible
1373A	10	27.8	0.9520	0.9511	0.9504	1.6	1.40	0.06	0.3	0.4	0.04	0.2	0.3	2.38	6.35	2.2	Thin dark scale over all surfaces	Some stain retained; machine marks visible
1374A	13	37.9	0.9515	0.9516	0.9510	0.5	1.40	0.02	0.1	0.1	0.01	0.1	0.1	3.13	4.89	1.7	Thin dull-black scale over all surfaces	Some stain retained; machine marks visible
1377A	18	19.2	0.9618	0.9637	0.9609	0.9	1.40	0.03	0.2	0.2	0.02	0.1	0.2	4.38	3.48	1.2	Thin dull-black scale over all surfaces	Some stain retained; machine marks visible
1379A	21	12.6	0.9609	0.9629	0.9602	0.7	1.40	0.02	0.1	0.2	0.02	0.1	0.1	5.13	2.76	1.0	Thin dull-black scale over all surfaces	Some stain retained; machine marks visible
1380A	22	11.2	0.9600	0.9620	0.9585	1.5	1.40	0.06	0.3	0.4	0.04	0.2	0.3	5.38	2.57	0.9	Thin dull-black scale over all surfaces	Same stain retained; machine marks visible
1381A	23	10.2	0.9657	0.9681	0.9652	0.5	1.40	0.02	0.1	0.1	0.01	0.1	0.1	5.63	2.39	0.8	Thin dull-black scale over all surfaces	Some stain retained; machine marks visible
1382A	24	9.3	0.9540	0.9563	0.9533	0.7	1.57	0.02	0.1	0.2	0.02	0.1	0.1	5.88	2.31	0.8	Thin dull-black scale over all surfaces	Same stain retained; machine marks visible
Zircaloy-2																		
Z 80	8	18.7	0.7936	0.7757	0.7759	17.1	1.40	0.74	3.9	5.2	0.50	2.6	3.5	1.88	7.35	2.5	Light-gray scale over all surfaces	Thin interference film retained; surfaces have slightly etched appearance
Z 81	11	32.6	0.8033	0.7893	0.7889	14.4	1.40	0.63	3.3	4.4	0.42	2.2	2.9	2.63	5.85	2.0	Light-gray scale over all surfaces	Thin film with some scattered flakes of scale retained on all surfaces
Z 82	14	41.9	0.7910	0.7786	0.7785	12.5	1.40	0.54	2.8	3.8	0.36	1.9	2.5	3.38	4.69	1.6	Light-gray scale over all surfaces	Very thin interference film retained; machine marks visible
Z 83	15	38.0	0.7913	0.7796	0.7794	11.9	1.40	0.52	2.7	3.6	0.35	1.8	2.4	3.63	4.32	1.5	Light-gray scale over all surfaces	Very thin interference film retained; machine marks visible
Z 84	20	14.2	0.7968	0.7866	0.7845	12.3	1.40	0.54	2.8	3.7	0.36	1.9	2.5	4.88	2.98	1.0	Light-gray scale over all surfaces	Very thin interference film retained; machine marks visible
Titanium-55A																		
Ti 145	6	14.1	0.5247	0.5236	0.5228	1.9	1.40	0.12	0.6	0.8	0.08	0.4	0.6	1.38	8.52	2.9	Thin brass-colored film on all surfaces	Clean; machine marks visible on all surfaces
Ti 157	9	22.1	0.5206	0.5201	0.5159	4.7	1.40	0.30	1.6	2.1	0.20	1.0	1.4	2.13	6.80	2.3	Thin brass-colored film on all surfaces	Some slight stain retained; most of the surface appears to be clean
Ti 159	12	34.9	0.5382	0.5378	0.5258	12.4	1.40	0.78	4.1	5.4	0.52	2.7	3.6	2.88	5.42	1.9	Thin brass-colored film on all surfaces	Some slight stain retained; most of the surface appears to be clean
Ti 161	16	28.3	0.5430	0.5430	0.5408	2.2	1.40	0.14	0.7	1.0	0.09	0.5	0.6	3.88	4.01	1.4	Thin brass-colored film on all surfaces	Some slight stain retained; machine marks visible
Ti 166	17	22.8	0.5358	0.5362	0.5333	2.5	1.40	0.16	0.8	1.1	0.11	0.6	0.7	4.13	3.72	1.3	Thin brass-colored film on all surfaces	Clean; machine marks visible
Ti 169	19	16.2	0.5270	0.5274	0.5250	2.0	1.40	0.12	0.7	0.9	0.08	0.4	0.6	4.63	3.21	1.1	Thin brass-colored film on all surfaces	Some slight stain retained; machine marks visible
3 Core Impact Specimens																		
Zircaloy-2 (total area each, 19.4 cm^2)																		
66	B		13.9076	13.5549		352.7	18.9	1.07	5.7	7.4	1.09	5.8	7.6	2.69	7.80	2.7	Thin dark-gray film with interference colors on all surfaces	
68	E		13.8562	13.5437		312.5	18.9	0.95	4.9	6.6	0.96	5.0	6.6	2.69	7.80	2.7	Thin dark-gray film with interference colors on all surfaces	
70	G		13.8789	13.5552		323.7	18.9	0.98	5.2	6.9	1.00	5.2	7.0	2.69	7.80	2.7	Thin dark-gray film with interference colors on all surfaces	
3 Core Tensile Specimens																		
Zircaloy-2																		
1-2	A		14.9044	14.5552		349.2	18.1	1.17	6.2	8.1	1.00	5.3	6.9	2.69	7.80	2.7	Thin light-gray film with interference colors on all surfaces	
13-14	C		14.9343	14.5756		358.7	18.1	1.20	6.4	8.3	1.02	5.5	7.1	2.69	7.80	2.7	Thin light-gray film with interference colors on all surfaces	
17-18	F		14.9183	14.5893		329.0	18.1	1.10	5.9	7.6	0.94	5.0	6.5	2.69	7.80	2.7	Thin light-gray film with interference colors on all surfaces	

[a]Two corrosion rates are presented: one based on the total operation time of 1672 hr and the other based on the total radiation time of 1255 hr (3 Mwhr of reactor time equivalent to 1 hr of total radiation time).

Table 11 (continued)

Sample Number	Position	Av Flow Velocity Across Specimen (fps)	Weight Data: Initial (g)	Weight Data: As Removed (g)	Weight Data: Defilmed (g)	Weight Data: Change (mg)	Exposed Sample Area (cm^2)	Corrosion Penetration (mils)	Corrosion Rate[a] (Exposed Area) (mpy): 1672 hr	Corrosion Rate[a] (Exposed Area) (mpy): 1255 hr	Corrosion Penetration (mils)	Corrosion Rate[a] (Total Area) (mpy): 1672 hr	Corrosion Rate[a] (Total Area) (mpy): 1255 hr	Distance from Front of First Specimen to Center of Specimen (in.)	Neutron Flux at Specimen Locations (neutrons/cm^2/sec x 10^{-12})	Power Density at Specimen Locations (w/ml)	As Removed	Defilmed
2 Core Rod Coupon Assemblies (18 coupons, 347 SS rods and spacers, total area each, 3.8 cm^2)																		
Stainless Steel Type 347																		
961A	1(A)		1.5985	1.5274	1.5264	72.1	3.4	0.94	4.9	6.6	0.84	4.4	5.9	1.42	10.48	3.6	Thin dark film on flat surfaces; brass-colored film on edges	Clean; lightly etched appearance; some machine marks visible
964A	3(B)		1.5997	1.5942	1.5933	6.4	3.4	0.08	0.4	0.6	0.07	0.4	0.5	2.13	8.90	3.1	Heavy brown rustlike scale over all surfaces	Clean; lightly etched appearance
962A	5(A)		1.6099	1.5527	1.5509	59.0	3.4	0.77	4.0	5.4	0.69	3.6	4.8	2.85	7.50	2.6	Thin dark film on flat surfaces; brass-colored film on edges	Clean; lightly etched on all exposed surfaces; more heavily etched in clamped area
965A	7(B)		1.6108	1.6114	1.6094	1.4	3.4	0.02	0.1	0.1	0.02	0.1	0.1	3.57	6.35	2.2	Heavy brown rustlike scale over all surfaces	Some stain retained; machine marks visible
966A	8(B)		1.6107	1.6120	1.6093	1.4	3.4	0.02	0.1	0.1	0.02	0.1	0.1	3.92	5.65	1.9	Heavy brown rustlike scale over all surfaces	Some stain retained; machine marks visible
963A	9(A)		1.6081	1.5804	1.5794	28.7	3.4	0.37	2.0	2.6	0.33	1.8	2.3	4.28	5.40	1.9	Thin dark film on flat surfaces; brass-colored film on edges	Clean; lightly etched on all exposed surfaces; more heavily etched in clamped area
Stainless Steel Type 309 SCb																		
C-1	2(A)		1.6115	1.5073	1.5047	106.8	3.4	1.40	7.3	9.7	1.25	6.5	8.7	1.78	9.60	3.3	One side covered with a heavy shiny black scale; the other with a thin dark film	Clean; lightly etched on all exposed surfaces; more heavily etched in clamped area
C-3	4(B)		1.5865	1.5810	1.5799	6.6	3.4	0.09	0.5	0.6	0.08	0.4	0.5	2.49	8.15	2.8	Heavy flaky brown rustlike scale on all surfaces	Clean; lightly etched on all exposed surfaces; more heavily etched in clamped area
C-2	6(A)		1.6262	1.5315	1.5297	86.5	3.4	1.13	5.9	7.9	1.01	5.3	7.0	3.21	6.90	2.4	One side covered with a heavy black scale; the other with a thin dark film	Some scale retained; generally cleon; lightly etched on all surfaces
C-4	9(B)		1.5976	1.5990	1.5965	1.1	3.4	0.02	0.1	0.1	0.01	0.1	0.1	4.28	5.39	1.9	Heavy brown rustlike scale on all surfaces	Some stoin retained; mochine marks visible
Zircaloy-2																		
Z 98	2(B)		1.2920	1.2107	1.2104	81.6	3.4	1.31	6.8	9.1	1.17	6.1	8.2	1.78	9.60	3.3	Heavy flaky brown rustlike scale on all surfoces	Uniform dark-gray film retained on rough surface
Z 96	4(A)		1.3245	1.2537	1.2526	71.9	3.4	1.15	6.0	8.0	1.03	5.4	7.2	2.49	8.15	2.8	Heovy flaky brown rustlike scale scattered on all surfoces	Uniform dark-gray film retained on rough surface
Z 99	6(B)		1.3170	1.2559	1.2559	61.1	3.4	0.98	5.1	6.8	0.88	4.6	6.1	3.21	6.90	2.4	Heavy light-gray scole over all surfaces	Uniform dark-gray film retained on rough surface
Z 97	8(A)		1.3393	1.2892	1.2886	50.7	3.4	0.81	4.3	5.7	0.73	3.8	5.1	3.92	5.39	1.9	Heavy flaky brown scale scattered over all surfaces	Uniform dark-gray film retained on rough surface
Platinum																		
Pt 3	1(B)		1.5656	1.5658	1.5647	0.9	3.4	0.005	0.03	0.03	0.004	0.02	0.03	1.42	10.48	3.6	Scottered flakes of brown scale over oll surfaces	Clean; some scratching from handling
Pt 1	3(A)		1.5570	1.5574	1.5568	0.2	3.4	0.001	<0.01	<0.01	0.001	<0.01	<0.01	2.13	8.90	3.1	Scattered flakes of brown scale over all surfaces	Clean; some scrotching from handling
Pt 4	5(B)		1.5662	1.5663	1.5661	0.1	3.4	<0.001	<0.01	<0.01	<0.001	<0.01	<0.01	2.85	7.50	2.6	Scattered flakes of brown scole over all surfaces	Clean; some scratching from handling
Pt 2	7(A)		1.5687	1.5701	1.5687	0.0	3.4	0	0	0	0	0	0	3.57	6.35	2.2	Scattered flakes of brown scale over all surfaces	Clean; some scratching from handling
24 In-Line Corrosion Sample Coupons (total areo each, 2.1 cm^2)																		
Stainless Steel Type 347																		
815A	1		8.9	0.9640	0.9672	0.9641	+0.1	1.57									Heavy dark-brown scale, uniform over all surfaces	Some black stain retained; machine marks visible
816A	2		9.5	0.9641	0.9677	0.9621	2.0	1.40	0.07	0.4	0.5	0.05	0.3	0.3			Heavy dark-brown scale, uniform over all surfaces	Some black stain retained; machine marks visible
980A	3		10.4	0.9568	0.9607	0.9565	0.3	1.40	0.001	0.1	0.1	0.006	<0.1	0.1			Heavy dark-brown scole, uniform over all surfaces	Some block stain retained; machine marks visible
986A	4		11.4	0.9588	0.9610	0.9584	0.4	1.40	0.002	0.1	0.1	0.01	0.1	0.1			Heavy dark-brown scale, uniform over all surfaces	Some black stain retained; machine marks visible
994A	5		12.7	0.9443	0.9492	0.9441	0.2	1.40	0.001	<0.1	0.1	0.006	<0.1	<0.1			Heavy dark-brown scale, uniform over all surfaces	Some black stain retained; machine marks visible
1118A	7		16.0	0.9606	0.9657	0.9598	0.8	1.40	0.03	0.2	0.2	0.02	0.1	0.1			Heavy dark-brown scale, uniform over all surfaces	Some black stain retained; machine marks visible
1119A	10		27.8	0.9520	0.9570	0.9509	1.1	1.40	0.04	0.2	0.3	0.02	0.1	0.2			Heavy dark-brown scale, uniform over all surfaces	Some black stain retained; machine marks visible
1120A	13		37.9	0.9560	0.9607	0.9556	0.4	1.40	0.002	0.1	0.1	0.01	0.1	0.1			Heavy dark-brown scale, uniform over all surfaces	Some black stain retained; machine marks visible
1124A	18		19.2	0.9558	0.9595	0.9556	0.2	1.40	0.001	<0.1	0.1	0.006	<0.1	<0.1			Heavy dark-brown scole, uniform over all surfaces	Some black stain retained; machine marks visible
1135A	21		12.6	0.9679	0.9713	0.9677	0.2	1.40	0.001	<0.1	0.1	0.006	<0.1	<0.1			Heavy dark-brown scale, uniform over all surfaces	Some black stain retained; machine marks visible
1136A	22		11.2	0.9508	0.9536	0.9493	1.1	1.40	0.04	0.2	0.3	0.02	0.1	0.2			Heavy dark-brown scale, uniform over all surfaces	Some black stain retained; machine marks visible
1138A	23		10.2	0.9653	0.9683	0.9640	1.3	1.40	0.05	0.2	0.3	0.03	0.2	0.2			Heavy dark-brown scale, uniform over all surfaces	Some black stain retained; machine marks visible
1139A	24		9.3	0.9540	0.9574	[b]		1.57									Heavy dark-brown scale, uniform over all surfaces	Some black stain retained; machine marks visible

[a]Two corrosion rates are presented: one based on the total operation time of 1672 hr and the other based on the total radiation time of 1255 hr (3 Mwhr of reactor time equivalent to 1 hr of total radiation time).
[b]Damaged in defilming.

Table 11 (continued)

Sample Number	Position	Av Flow Velocity Across Specimen (fps)	Weight Data: Initial (g)	Weight Data: As Removed (g)	Weight Data: Defilmed (g)	Weight Data: Change (mg)	Exposed Sample Area (cm^2)	Corrosion Penetration (mils)	Corrosion Rate[a] (Exposed Area) (mpy): 1672 hr	Corrosion Rate[a] (Exposed Area) (mpy): 1255 hr	Corrosion Penetration (mils)	Corrosion Rate[a] (Total Area) (mpy): 1672 hr	Corrosion Rate[a] (Total Area) (mpy): 1255 hr	Distance from Front of First Specimen to Center of Specimen (in.)	Neutron Flux at Specimen Locations (neutrons/cm^2/sec x 10^{-12})	Power Density at Specimen Locations (w/ml)	As Removed	Defilmed
														Zircaloy-2				
Z 75	8	18.7	0.7861	0.7908	0.7864	+0.3	1.40										Heavy dark-brown scale, uniform over all surfaces	Scattered flakes of scale retained on all surfaces; machine marks visible
Z 76	11	32.6	0.8089	0.8132	0.8088	0.1	1.40										Heavy dark-brown scale, uniform over all surfaces	Scattered flakes of scale retained on all surfaces; machine marks visible
Z 77	14	41.9	0.7888	0.7930	0.7889	+0.1	1.40										Heavy dark-brown scale, uniform over all surfaces	Scattered flakes of scale retained on all surfaces; machine marks visible
Z 78	15	38.0	0.7951	0.7990	0.7951	0.0	1.40	0.0	0.0	0.0	0.00	0.00	0.00				Heavy dark-brown scale, uniform over all surfaces	Scattered flakes of scale retained on all surfaces; machine marks visible
Z 79	20	14.2	0.7860	0.7895	0.7861	+0.1	1.40										Heavy dark-brown scale, uniform over all surfaces	Scattered flakes of scale retained on all surfaces; machine marks visible
														Titanium-55A				
Ti 109	6	14.1	0.5311	0.5366	0.5297	1.4	1.40	0.09	0.5	0.6	0.06	0.3	0.4				Heavy dark-brown scale, uniform over all surfaces	Very thin light-brown stain retained; machine marks visible
Ti 115	9	22.1	0.5271	0.5321	0.5240	3.1	1.40	0.20	1.0	1.4	0.13	0.7	0.9				Heavy dark-brown scale, uniform over all surfaces	Very thin light-brown stain retained; machine marks visible
Ti 117	12	34.9	0.5286	0.5330	0.5281	0.5	1.40	0.03	0.2	0.2	0.02	0.1	0.1				Heavy dark-brown scale, uniform over all surfaces	Very thin light-brown stain retained; machine marks visible
Ti 125	16	28.3	0.5365	0.5411	0.5351	1.4	1.40	0.09	0.5	0.6	0.06	0.3	0.4				Heavy dark-brown scale, uniform over all surfaces	Very thin light-brown stain retained; machine marks visible
Ti 139	17	22.8	0.5365	0.5403	0.5349	1.6	1.40	0.10	0.5	0.7	0.07	0.4	0.5				Heavy dark-brown scale, uniform over all surfaces	Very thin light-brown stain retained; machine marks visible
Ti 141	19	16.2	0.5355	0.5384	0.5295	6.0	1.40	0.38	2.0	2.6	0.25	1.3	1.8				Heavy dark-brown scale, uniform over all surfaces	Very thin light-brown stain retained; machine marks visible
														3 Special In-Line Impact Specimens (total area each, 19.4 cm^2)				
														Zircaloy-2				
60	B		13.8377	13.8613		+23.6	18.9										Heavy black scale, uniform over all surfaces	
62	D		13.7822	18.8074		+25.2	18.9										Heavy black scale, uniform over all surfaces	
64	F		13.8602	13.8850		+24.8	18.9										Heavy black scale, uniform over all surfaces	
														3 Special In-Line Tensile Specimens (total area each, 21.2 cm^2)				
														Zircaloy-2				
5-6	A		14.9742	14.9980		+23.8	18.1										Heavy black scale, uniform over all surfaces	
9-10	C		14.9834	15.0052		+21.8	18.1										Heavy black scale, uniform over all surfaces	
21-22	E		14.9699	14.9930		+23.1	18.1										Heavy black scale, uniform over all surfaces	
														Core Coupon Holder No. 8 (total area each, 160.0 cm^2)				
														Stainless Steel Type 347				
A			98.3703	98.2340	98.1768	193.5	~160.0										Brass-colored film over front half, gradually changing to a black velvety scale on remainder	Some stain retained; machine marks visible
B			99.3743	(This Half Damaged)			~160.0										Damaged in removal operations	
														In-Line Coupon Holder No. 7 (total area each, 160.0 cm^2)				
														Stainless Steel Type 347				
A			114.5164	114.6385	114.4713	45.1	~160.0										Heavy dark-brown scale over all surfaces, somewhat thinner on outside	Some scattered flakes of scale; machine marks visible
B			117.2574	(This Half Damaged)			~160.0										Damaged in removal operations	

[a]Two corrosion rates are presented: one based on the total operation time of 1672 hr and the other based on the total radiation time of 1255 hr (3 Mwhr of reactor time equivalent to 1 hr of total radiation time).

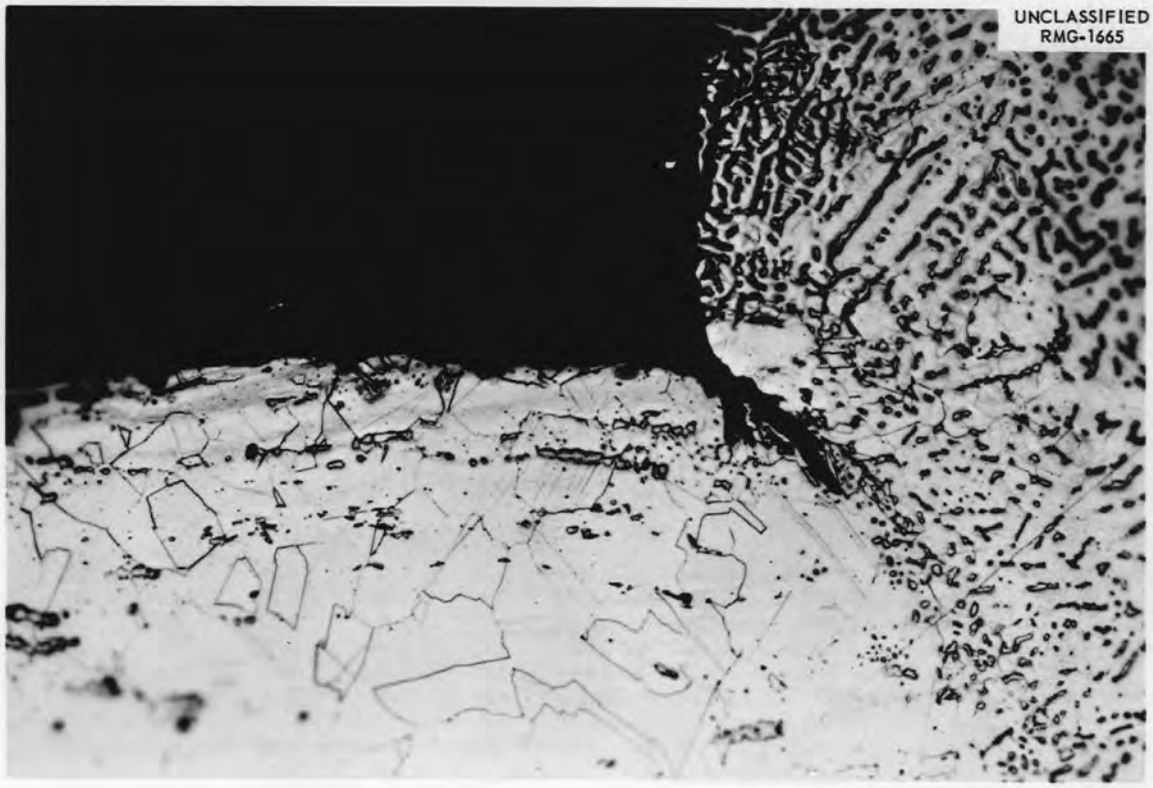

Fig. 16. Pump Outlet Piping. 250X. Reduced 11%.

neutron flux to which a given core specimen was exposed during operation and the corresponding fission power density in solution are also listed. The flux values are those which correspond to the specimen positions in the core as shown by the stainless steel–Zircaloy-2 curves on the flux-vs-position plot in Fig. 8. Those for the impact and tensile specimens were obtained by averaging logarithmically the flux values at the ends of each. Table 13 lists the factors used in computing corrosion penetration from weight losses.

Corrosion-rate values for Zircaloy-2 and titanium-55A reported below were calculated from weight-loss data with the total specimen area and radiation time (where 3 Mwhr of reactor energy is equal to 1 hr of total radiation time) used as bases. Those for steel are based on exposed area and radiation time. Average solution velocities across the coupons contained in the tapered-channel core and in-line holders were from 9 to 42 fps. Solution velocity across the core-annulus specimens was approximately 1 fps. The core channel and core annulus specimens are designated CC and CA, respectively.

Zircaloy-2. – Corrosion rates observed for the five Zircaloy-2 core-channel (CC) coupons varied from 2.5 mpy at 1 w/ml solution fission power density to 3.5 mpy at 2.5 w/ml. The solution velocity across these coupons varied from 14 to 42 fps, as shown in Fig. 1. Corrosion rates observed for the four Zircaloy-2 core-annulus (CA) rod-type coupons varied from 5.1 mpy at 1.9 w/ml to 8.2 mpy at 3.3 w/ml. Corrosion rates for the three "as-machined" Zircaloy-2 CA impact and three "as-machined" Zircaloy-2

Table 12. Summary of Metallographic Examination of Corrosion Coupans

Coupon Number	Position	Avg Thickness Measurement (in.)	Metallographic Observations
		Type 347 Stainless Steel	
1245A	Core channel 2	0.059	A few isolated pits on sides; one end rough
1373A	Core channel 10	0.060	Sides smooth; both ends rough and pitted
1381A	Core channel 23	0.061	Two or three pits on sides; one end rough
962A	Core annulus A-5	0.059	Slight isolated pitting on sides and end
964A	Core annulus B-3	0.060	Slight isolated pitting on sides and ends
		Type 309 SCb Stainless Steel	
C-1	Core annulus A-2	0.057	Rough, uneven surface; slight pitting
C-4	Core annulus B-9	0.059	A few small cracks (<2 mils) near center on one side; two or three isolated pits; otherwise smooth
		Titanium-55A	
Ti-139	In-line channel 17	0.059	Smooth, no attack
Ti-141	In-line channel 19	0.058	Sides smooth; one end slightly roughened
Ti-145	Core channel 6	0.057	Sides smooth; one corner slightly roughened
Ti-159	Core channel 12	0.055	Pits (< ½ mil deep) near center of one side; otherwise smooth
		Zircaloy-2	
Z-82	Core channel 14	0.060	Sides slightly roughened; ends smooth; one corner eroded
Z-84	Core channel 20	0.059	Sides roughened less than Z-82; ends smooth
Z-97	Core annulus A-8	0.058	All surface roughened; no localized attack evident
Z-77	In-line channel 14	0.060	All surfaces smooth; no film visible

Table 13. Corrosion Penetration Factors

Material	Density (g/cm^3)	Factor (mg of material per cm^2 per mil penetration)
Type 347 stainless steel	8.02	20.37
Type 309 SCb stainless steel	8.02	20.37
Zircaloy-2	6.5	16.51
Titanium-55A	4.54	11.53
Platinum	21.45	54.48

tensile specimens, based on "as-removed" weight changes, were observed to vary from 6.6 to 7.6 mpy and 6.5 to 7.1 mpy respectively. All six of these specimens were exposed to the same average solution fission power density, 2.7 w/ml. Although the impact and tensile specimens were not defilmed, it is believed that little scale was retained and that the corrosion rates are reliable. As shown in Table 11 cathodic defilming of other "as-removed" Zircaloy-2 specimens resulted in very small weight changes. The above data are given in Table 11 and are shown in Fig. 17 as a plot of corrosion rate vs the solution fission power density at the specimen positions. Shown for comparison is the range of corrosion rates observed for the Zircaloy-2 core coupons from all previous in-pile loop experiments.[9] As mentioned above, these previous loop experiments were exposed in the LITR beam hole HB-4 with 0.17 *m* UO_2SO_4 solutions at 250°C.

Zircaloy-2 CC coupon Z-81 and CA coupon Z-98 were submitted for analysis for hydrogen content after the usual defilming procedure. The specimens were reported to have contained 44 and 23 ppm H_2, respectively, quantities approximating the nominal content for Zircaloy-2 material.[10] The estimated pressure of radiolytic gas in the main-stream solution, in which these coupons were immersed, was about 30 psi.

UNCLASSIFIED
ORNL-LR-DWG 64023

EXPERIMENT NO.				APPROXIMATE CONDITIONS FOR LOOP EXPERIMENTS					
				SOLUTION COMPOSITION (*m*)					TEMPERATURE (°C)
						H_2SO_4			
CC	CA	IMPACT	TENSILE	UO_2SO_4	$CuSO_4$	ORIGINAL SOLUTION	MAKE-UP	MEAN	
FF				0.17	0.03	0.04	0.04	0.028	250
GG				0.17	0.03	0.04	0.04	0.026	250
L-4-8				0.17	0.03	0.04	0.04	0.023	250
L-4-11				0.17	0.03	0.04	0.04	0.022	250
L-4-12				0.17	0.03	0.04	0.04	0.031	250
EE				0.17	0.03	0.008	0.04	0.006	250
● L-2-10	○	△	▲	0.04	0.008	0.02	0.04	0.018	280

NOTE: IMPACT AND TENSILE SPECIMENS WERE NOT DEFILMED

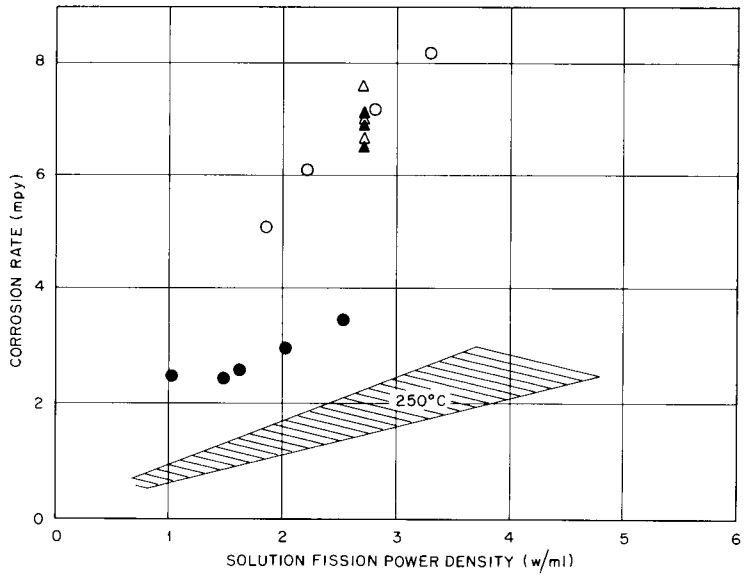

Fig. 17. Corrosion of Zircaloy-2.

With the exception of one coupon, all in-line channel coupons from L-2-10 showed either no weight change or weight increases following defilming. These increases ranged from 0 to 1.5 mg/cm^2. The exception, a coupon exposed to an average solution velocity of 33 fps, exhibited a weight loss following defilming corresponding to about a 0.02-mpy corrosion rate. All six in-line tensile and impact specimens exhibited weight increases, in the "as-removed" condition, of from 0.9 to 1.1 mg/cm^2.

Titanium-55A. – Corrosion rates of 1.4 and 3.6 mpy were observed for two of the six titanium-55A CC coupons. These specimens were exposed to solution fission power densities of 2.3 and 1.9 w/ml, and the average solution velocities across the coupons were 22 and 35 fps. Corrosion rates for the other four coupons were all less than 1 mpy. These specimens were exposed to solution fission power densities ranging from 1.1 to 2.9 w/ml and solution velocities ranging from 14 to 28 fps. The average rate for the six coupons was 1.2 mpy. There were no CA coupons of this material in the experiment.

Corrosion rates for the six Ti-55A in-line channel coupons were observed to vary from 0.1 to 1.8 mpy. The average solution velocity across these coupons also varied from 14 to 35 fps. These data are given in Table 11. The corrosion rate data for the CC coupons are compared in Fig. 18, as a plot of corrosion rate vs solution fission power density, with those obtained previously for Ti-55A CC coupons in the HB-4 experiments, EE, L-4-8, and L-4-12.[11] Also shown are the corrosion rate data for the Ti-110AT and Ti-130AM core coupons exposed in loop L-4-11.[2]

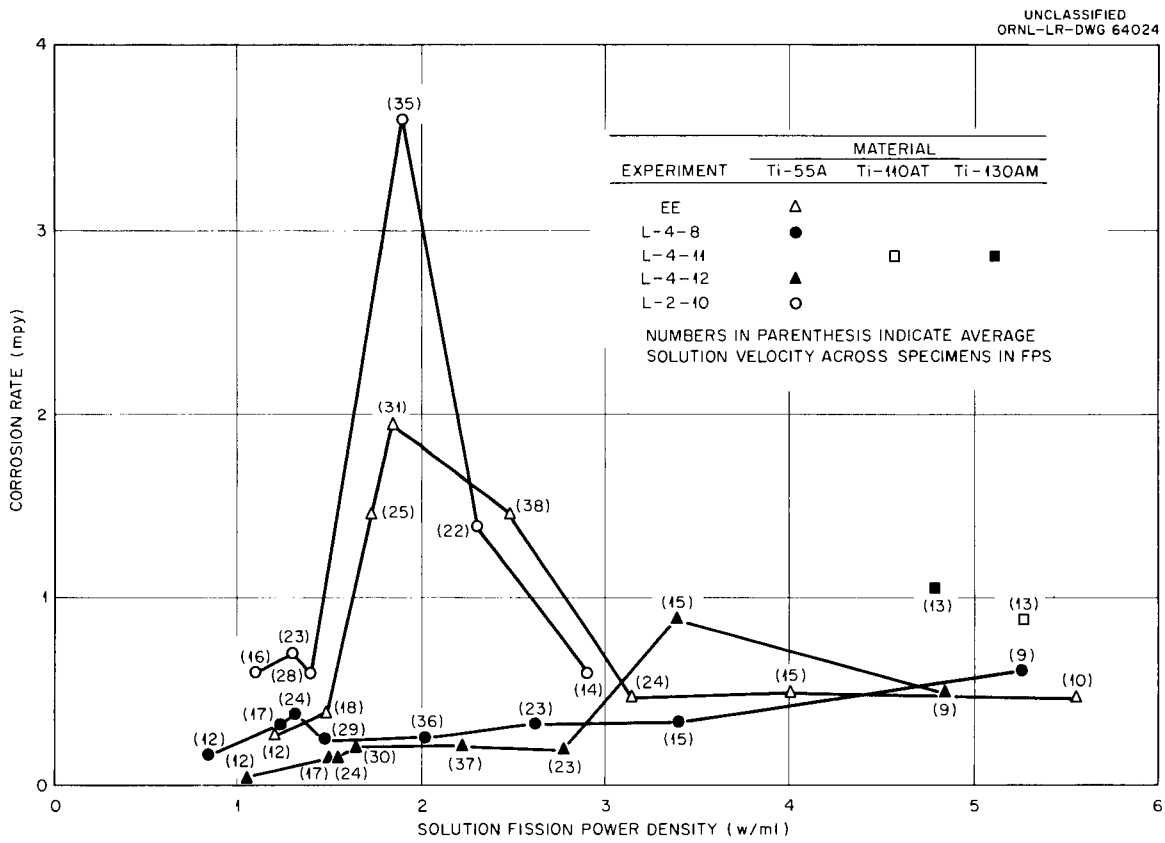

Fig. 18. Corrosion of Titanium-55A Core Channel Coupons.

Platinum. – The four platinum CA rod coupons corroded very slightly. The observed rates varied from 0 mpy at 2.4 w/ml solution fission power density to 0.03 mpy at 3.6 w/ml. There were no platinum specimens in the line channel coupon array. All core specimens were clean and shiny when weighed. Cathodic defilming appeared to have removed all traces of film, and the corrosion results are considered reliable within the weighing limitations (± 0.2 mg/cm^2). These data are given in Table 11.

Types 347 and 309 SCb Stainless Steel. – Corrosion rates for the 13 type 347 stainless steel CC coupons varied from 0.2 mpy at 0.8 w/ml solution fission power density to 2.8 mpy at 4.2 w/ml. The average solution velocity across these specimens varied from 9 to 38 fps. These data are given in Table 11 and are shown in Fig. 19. The average solution velocity past a given specimen is indicated in the plot in parentheses where it was greater than ~ 1.

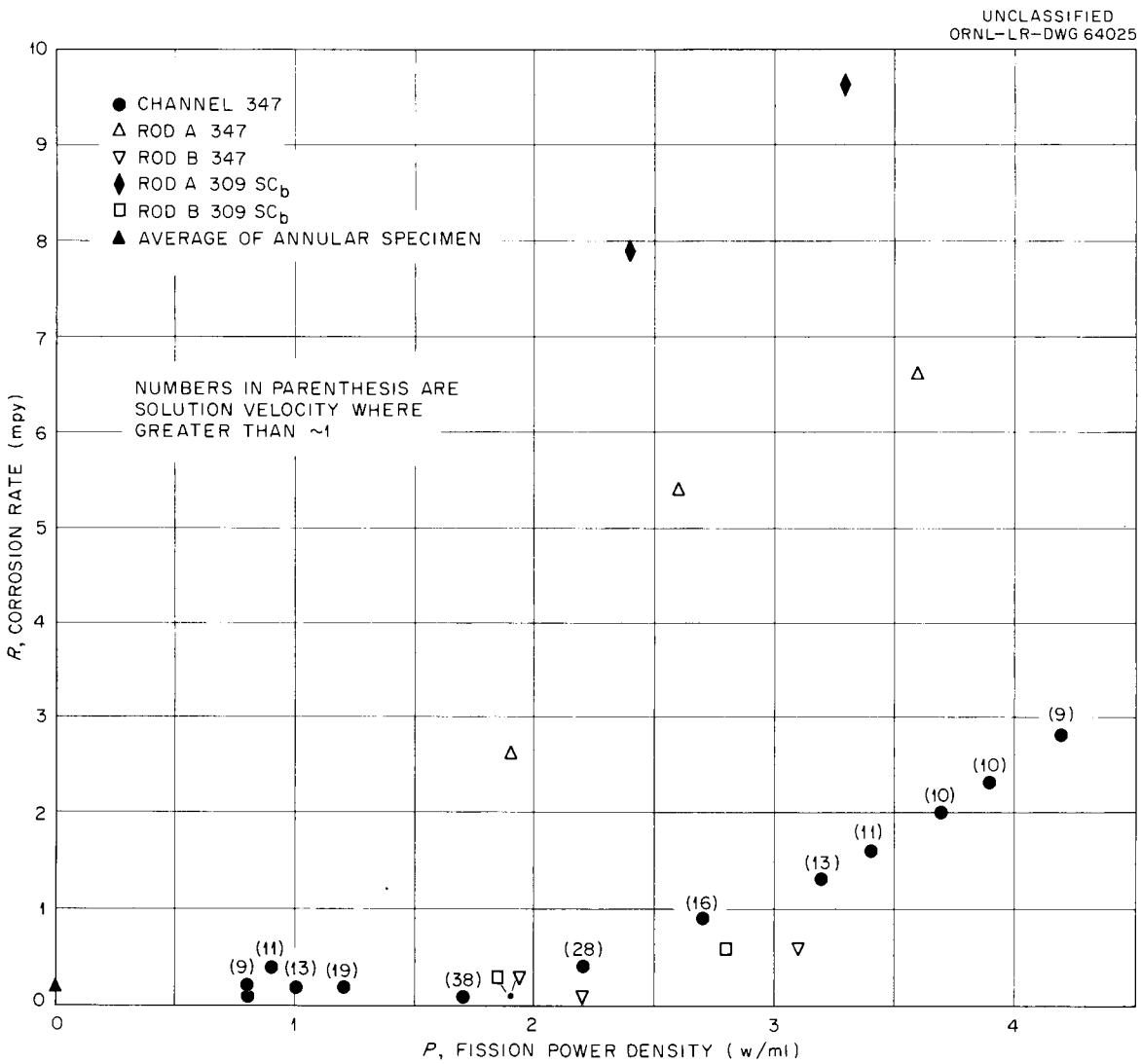

Fig. 19. Steel Corrosion, In-Pile Loop L-2-10.

Three rod coupons of type 347 stainless steel, contained in CA coupon assembly B, exhibited corrosion rates that were about the same or somewhat less than those observed for the CC coupons. The three specimens on the other rod coupon assembly, A, in the core annulus exhibited appreciably higher rates: from 2.6 mpy at 1.9 w/ml to 6.6 mpy at 3.6 w/ml solution fission power density. Each rod coupon assembly also contained two coupons of type 309 SCb stainless steel. The observed corrosion rates for these specimens were, in each assembly, somewhat greater than those exhibited by the type 347 stainless steel rod coupons. These data are given in Table 11 and are shown in Fig. 19.

The in-line channel specimens of type 347 stainless steel exhibited a maximum rate of 0.45 mpy, and the average rate for the 13 specimens was 0.18 mpy. The rates for these specimens were not affected by variation in the average solution velocity from 9 to 38 fps. The average rate value is plotted in Fig. 19 at zero power density.

5. SUMMARY AND DISCUSSION OF RESULTS

5.1 Zircaloy-2

The Zircaloy-2 data have been analyzed and included in a general discussion of Zircaloy-2 radiation-corrosion effects by Jenks.[12] For convenience, the conclusions from that discussion which are pertinent to the present experiment will be summarized here.

As reported by Jenks, the Zircaloy-2 data from this experiment, as well as all other 280°C in-pile loop and autoclave experiments, can be expressed by the following equation:

$$1/R = 2.23/P\alpha + 1/K \ , \qquad (1)$$

where

R = corrosion rate, mpy,

P = fission power density in solution, w/ml,

K = 40 mpy,

α = factor by which the effective power density is greater than the solution power density due to uranium sorption near or on the corroding surface and which varies only with solution composition and solution velocity.

Average corrosion rates (based on total specimen area and length of exposure at 3 Mw) for the five CC and four CA coupons contained in this experiment are shown in Fig. 20 as a plot of the reciprocal of corrosion rate vs the reciprocal of solution fission power density. Shown for comparison is a line representing the Zircaloy-2 CC and CA corrosion data from two subsequent 280°C experiments, L-2-14[7] (0.17 *m* UO_2SO_4, 0.15 *m* $CuSO_4$, 0.4 *m* H_2SO_4) and L-2-19[13] (0.17 *m* UO_2SO_4, 0.02 *m* $CuSO_4$, 0.10 *m* H_2SO_4, 0.20 *m* Li_2SO_4). There was probably a negligible effect from sorbed uranium on the specimens from experiments L-2-14 and L-2-19, and hence an α value of 1 was assumed for these data.[12] As shown in Fig. 20, the data from these two experiments extrapolated to a value of 40 mpy at infinite power density, and the CA data from the present experiment also fall near the straight line which is drawn arbitrarily through the

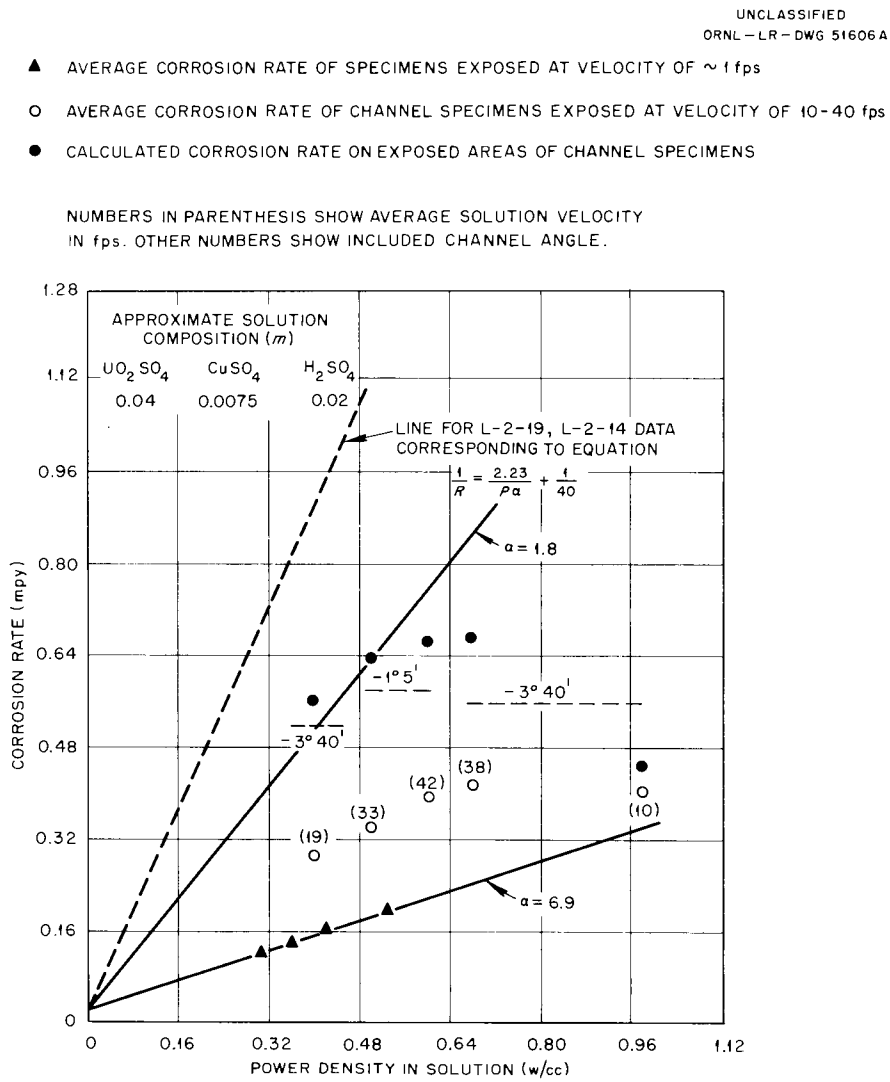

Fig. 20. Corrosion of Zircaloy-2 at 280°C.

same point on the ordinate. The value of 6.9 for α was calculated by employing Eq. (1). It was estimated from comparisons with the results of analyses of specimens from a subsequent experiment, L-2-17,[14] that the low-velocity (~1 fps) CA coupons in the present experiment sorbed about 20 μg of uranium per cm^2. In the absence of any heavy scale the calculated α value for this amount of sorbed uranium and for a 0.04 *m* UO_2SO_4 solution is about 6, based on fission-recoil energy deposition; and on this basis the experimental value of 6.9 for α for these specimens appears reasonable.

As shown in Fig. 20, the average corrosion rates exhibited by the Zircaloy-2 CC specimens were appreciably less than the rates observed for the CA specimens. This difference is ascribed to a beneficial velocity effect in which the amounts of sorbed uranium are reduced by the rapid flow of solution past surfaces. The average rates plotted were calculated by assuming that the corrosion penetration indicated by a

specimen weight loss was uniform over the entire surface of the specimen. However, it appears probable[12] that as a result of lower velocities past covered surfaces, the uranium sorption (and hence the corrosion rates) was greater on covered than on exposed surfaces. Estimated corrosion rates for the exposed portions of the CC coupons were calculated by assuming equality between the rates on covered surfaces and on the low-velocity CA specimens at the same power densities. The resulting values, represented by the circles in Fig. 20, are lower than the average rates but are still greater than those expected for $\alpha = 1$ (L-2-14 and L-2-19). However, the proper correction for corrosion on covered surfaces is uncertain, and it is possible that an α value of 1 prevailed for the high-velocity specimen in the convergent section of the channel.

The ratio of the solution velocity at the wall to that in the center of channel holders such as those employed in this experiment depends upon the included angle and decreases with increasing values of the angle.[12] The removal of uranium or other material from a specimen surface probably depends upon the velocity near the surface, and thus it is expected that the beneficial effects of a given average solution velocity decrease with increasing value of the angle. This is assumed to be the explanation for the relatively high α value exhibited by the specimens in the divergent section of the holder.

It should also be mentioned, although not shown in Fig. 20, that the corrosion rates observed for the impact and tensile specimens located in the core annulus are in close agreement with those for the CA coupons at similar power densities and the same average velocity.

As mentioned above, the in-line coupons were covered with scale in the "as-removed" condition. However, as shown in Table 11, differences in the "as-removed" and defilmed weights for these coupons varied from only 1.2 to 0.9 mg/cm^2. Zircaloy-2 in-line specimens from previous in-pile loop experiments have exhibited greater scale retention. The coupons from this experiment exhibited either very slight corrosion rates or weight increases following defilming.

5.2 Titanium-55A

The results obtained with Ti-55A coupons in this experiment show that, with the exception of the one channel specimen which was exposed to a high velocity (Fig. 18), the CC specimens corroded at about the same average rates as the LC (in-line) specimens (0.7 mpy average in-line vs 0.8 mpy average CC excluding the one high-rate specimen). Also, no significant effect of local solution fission power density on the corrosion rates of the CC specimens was apparent. For this experiment, the in-line and low-power-density specimens apparently had only very small amounts of retained scale, so that the rates calculated from the results of weight measurements are considered exceptionally reliable. The conclusions regarding the in-pile corrosion of titanium which are drawn from these results are:

1. The corrosion of titanium is accelerated during in-pile exposure by some change which occurs throughout the solution under irradiation, so that surfaces in and out of the core are affected to about the same extent.
2. Fission-recoil irradiation of a surface, as well as direct exposure to solution in which fission is occurring, has no appreciable effect on the rate except that the susceptibility to an adverse velocity effect may be increased.

These conclusions are not supported entirely by the data obtained in prior 250°C loop experiments shown in Fig. 18. The general trend of these prior data indicate a small increase in rate with increasing power density. However, at the generally low rates prevailing for titanium, it is likely that the previous results were affected appreciably by retained scale. Since there was usually more retained scale on surfaces near the rear of the core (low power densities) and at in-line positions than at the front of the core, the lower-power-density specimens may have exhibited less weight loss (lower calculated rate) than the high-power-density specimens at the same corrosion rate. It may be noted that results obtained in subsequent 280°C loop experiments L-4-16 and L-2-15[15] support the above conclusions.

It should be pointed out that the rate values plotted in Fig. 18 are based on total area. For those specimens which were adversely affected by solution velocity, the rates on the exposed surfaces were probably nearer those calculated using exposed rather than total area, since the covered surfaces of a specimen were exposed to essentially stagnant solution. The calculated rates based on exposed areas are listed in Table 11. They are about 60% greater than the total-area rates.

5.3 Stainless Steel

In general, steel corrosion in the core of the different experiments has shown some wide variations, and no correlations of data have been accomplished from which steel behavior under a given set of conditions can be confidently anticipated. The in-line steel corrosion in loops has been consistently low and about the same as that found in out-of-pile exposure. Corrosion in the core is influenced by the reactor radiations.

Over-all Corrosion Rate of Steel, from Oxygen and Nickel Data. – The average over-all rate of steel corrosion in the loops was 0.35 mpy based on oxygen uptake data, 1672 hr of in-pile operation, and total area of steel wetted by high-temperature solution. Based on data for nickel in solution, the comparably calculated value was 0.2 mpy. On the basis of radiation time of 1252 hr, the over-all rates were 0.47 and 0.27 mpy from oxygen and nickel data respectively. Both oxygen and nickel data indicated that the actual corrosion rates decreased slightly during the course of the exposure, the nickel data indicating the greater decrease. No appreciable differences were noted between rates of oxygen uptake during reactor up and down periods. However, the latter were of relatively short duration, and the rates during these periods were not accurately determined. Nickel data for the corrosion during down periods were obtained only during the 190-hr period prior to the initiation of irradiation. During this period, the amounts of corrosion determined from oxygen and nickel data were in near agreement.

An estimate of the total steel corrosion based on specimen weight losses in the core and in-line positions has been made, but the result is considered to be of small significance because of the wide differences in corrosion between the specimens located in different portions of the core and the resulting uncertainty in the estimate of the corrosion suffered by the core walls. This estimate of total steel corrosion was made as follows: It was assumed that the core channel coupon holder corroded at the average rate calculated for the type 347 stainless steel CA coupons, and that pressurizer, pressurizer lines, pump,

main circulation lines, in-line stainless steel fittings, and in-line channel coupon holders corroded at the same average rate as the LC coupons. On this basis the total stainless steel weight loss in the experiment was computed to be 7.8 g, which is equivalent to about 2340 cc(STP) of oxygen.

During in-pile exposure 1730 cc of oxygen was taken up by processes other than corrosion of titanium and zirconium alloys. An additional volume of about 850 cc was taken up during preparatory operations. Thus, if it is assumed that oxygen was taken up only in corrosion, the oxygen data show that 8.6 g of steel was oxidized, an amount about 10% greater than that estimated from specimen weight data. The nickel data indicate a total of about 6.8 g of steel oxidized during the preparatory and in-pile operations (2.8 and 4.0 g, respectively).

The difference between the values for steel oxidation determined from nickel and oxygen data is probably explained by loss of nickel from the solutions resulting from sorption of this element on the various corrosion product oxides. Analyses of scales recovered from subsequent loop experiments have shown that nickel is a constituent of the scales.[13]

Corrosion of Steel in Regions Outside the Core. – The maximum corrosion rate of steel specimens in the in-line channel positions was 0.45 mpy, and the average rate for the 13 specimens was 0.18 mpy (based on radiation time and exposed area). These rates were not affected by variations in average solution velocity from 9 to 38 fps. Metallographic and visual examinations did not reveal any areas of significant localized attack outside the core, and there is no reason to suspect that localized corrosion attack occurred at some undetected location.

Corrosion of Steel in the Core. – The plot of the core-specimen data shown in Fig. 19 shows that the average rate of attack of those channel specimens exposed to power densities above about 2 w/ml increased with increasing fission power density in an apparently regular fashion. Below about 2 w/ml, the rates were near those for the in-line channel specimens. No effect of varying solution velocities in the range 9 to 38 fps is apparent for these CC specimens.

As also shown in Fig. 19, the type 347 and 309 SCb steel specimens on rod A corroded at much higher rates than the channel specimen, while those on rod B corroded at somewhat lower rates. Explanations that have been considered for these differences include differences in (1) temperature, (2) uranium sorption due to differences in solution velocity, (3) galvanic effects, and (4) solution composition. Explanations (1) and (2) are believed unlikely, because Zircaloy-2 specimens located on the two different holders corroded at similar rates at similar power densities. Zircaloy-2 corrosion is sensitive to the temperature and amounts of uranium sorbed, and it seems unlikely that the temperature and sorption conditions could have differed enough to influence relative corrosion of steel without affecting the relative corrosion of Zircaloy-2. Explanation (4) was considered because the probable flow pattern was one in which entering solution contacted specimens in the upper half of the core (rod B) before reaching those in the lower half (rod A). The solution bathing specimens on rod B would thus contain lower concentrations of some short-lived fission products than that bathing rod A. This explanation is now believed unlikely because of the consideration that while channel specimens were exposed to solution which must have had long core residence times on the average, their rates were no greater than those on rod B. Explanation (3) appears the most likely at

present, although the mechanism causing a difference in galvanic action between the specimens on the two different holders is not understood. (Each array included equal numbers but different arrangements of specimens of platinum and stainless steels.)

5.4 Solution Stability

Some rather wide fluctuations occurred in the reported concentration of various solutes. It is believed that these resulted from sampling and analytical errors. No evidence of solution instability was apparent within the probable accuracy of the data.

REFERENCES

1. J. E. Baker and G. H. Jenks, *HRP Radiation Corrosion Studies: In-Pile Loop L-4-8*, ORNL-2042 (Aug. 8, 1956).
2. J. R. McWherter and J. E. Baker, *HRP Radiation Corrosion Studies: In-Pile Loop L-4-11*, ORNL-2152 (June 11, 1958).
3. H. C. Savage *et al.*, *In-Pile Corrosion Test Loops for Aqueous Homogeneous Reactor Solutions*, ORNL-2977 (Dec. 21, 1960).
4. F. J. Walter, *HRP In-Pile Corrosion Test Loops – Operation of In-Pile Loop L-2-10*, ORNL CF-57-6-49.
5. Personal communication from J. O. Stiegler.
6. G. M. Adamson *et al.*, *HRP Quart. Progr. Rept. July 31, 1957*, ORNL-2379, p 127.
7. G. H. Jenks and J. E. Baker, *HRP Radiation Corrosion Studies: In-Pile Loop L-2-14*, ORNL-2943 (in press).
8. G. H. Jenks and J. E. Baker, *Apparent Copper Rate Constants Determined in In-Pile Loop Experiment L-2-22*, ORNL CF-60-3-88 (Mar. 23, 1960).
9. G. H. Jenks *et al.*, *HRP Quart. Progr. Rept. Oct. 31, 1956*, ORNL-2222, p 104.
10. Nucleonics Data Sheet No. 30, *Nucleonics*, p 72, March 1959.
11. G. H. Jenks *et al.*, *HRP Quart. Progr. Rept. Oct. 31, 1956*, ORNL-2222, p 103.
12. G. H. Jenks, *A Model for the Effects of Irradiation on Zircaloy-2 Corrosion and a Review and Correlation of In-Pile Zircaloy-2 Corrosion Data*, ORNL-3039 (July 6, 1961).
13. G. H. Jenks and J. E. Baker, *HRP Radiation Corrosion Studies: In-Pile Loop L-2-19*, ORNL-2953 (in press).
14. G. H. Jenks *et al.*, *HRP Quart. Progr. Rept. Jan. 31, 1958*, ORNL-2493, p 124.
15. G. H. Jenks *et al.*, *HRP Quart. Progr. Rept. July 31, 1957*, ORNL-2379, p 110.

ORNL-2962
UC-25 – Metals, Ceramics, and Materials
(TID-4500 17th ed.)

INTERNAL DISTRIBUTION

1. G. M. Adamson
2. A. L. Bacarella
3. J. E. Baker
4. J. M. Baker
5. S. E. Beall
6. D. S. Billington
7. F. F. Blankenship
8. A. L. Boch
9. E. G. Bohlmann
10. S. E. Bolt
11. G. E. Boyd
12. R. B. Briggs
13. W. D. Burch
14. E. L. Compere
15. F. L. Culler
16. R. J. Davis
17. V. A. DeCarlo
18. J. L. English
19. D. E. Ferguson
20. J. H. Frye, Jr.
21. W. R. Gall
22. J. C. Griess
23. W. R. Grimes
24. P. N. Haubenreich
25. J. W. Hill, Jr.
26. G. H. Jenks
27. R. G. Jordan (Y-12)
28. W. H. Jordan
29. M. T. Kelley
30. M. J. Kelly
31. R. B. Korsmeyer
32. J. A. Lane
33. C. E. Larson
34. C. G. Lawson
35. R. A. Lorenz
36. R. N. Lyon
37. W. D. Manly
38. W. L. Marshall
39. J. P. McBride
40. H. G. MacPherson
41. R. E. McDonald
42. H. F. McDuffie
43. J. R. McWherter
44. J. P. Murray (K-25)
45. A. R. Olsen
46. M. L. Picklesimer
47. H. C. Savage
48. C. H. Secoy
49. M. J. Skinner
50. I. Spiewak
51. J. A. Swartout
52. A. Taboada
53. E. H. Taylor
54. G. M. Watson
55. A. M. Weinberg
56. J. C. White
57. Biology Library

58–59. Central Research Library
60. Reactor Division Library
61–80. Laboratory Records Department
81. Laboratory Records, ORNL RC
82. ORNL – Y-12 Technical Library, Document Reference Section
83. F. Daniels (consultant)
84. F. T. Gucker (consultant)
85. F. T. Miles (consultant)

EXTERNAL DISTRIBUTION

86. Division of Research and Development, AEC, Washington
87. Division of Research and Development, AEC, ORO
88. Division of Reactor Development, AEC, Washington
89. Division of Reactor Development, AEC, ORO

90–658. Given distribution as shown in TID-4500 (17th ed.) under Metals, Ceramics, and Materials category (75 copies – OTS)